

## Article

# Optimal Design and Operation of an Off-Grid Hybrid Renewable Energy System in Nigeria's Rural Residential Area, Using Fuzzy Logic and Optimization Techniques

Taofeek Afolabi and Hooman Farzaneh \* 

Interdisciplinary Graduate School of Engineering Sciences, Kyushu University, Fukuoka 816-8580, Japan

\* Correspondence: farzaneh.hooman.961@m.kyushu-u.ac.jp

**Abstract:** This study focuses on a technical and economic analysis of designing and operating an off-grid hybrid renewable energy system (HRES) in a rural community called Olooji, situated in Ogun state, Nigeria, as a case study. First, a size optimization model is developed on the basis of the novel metaheuristic particle swarm optimization (PSO) technique to determine the optimal configuration of the proposed off-grid system on the basis of the minimization of the levelized cost of electricity, by factoring in the local meteorological and electricity load data and details on the technical specification of the main components of the HRES. Second, a fuzzy-logic-controlled energy management system (EMS) is developed for the dynamic power control and energy storage of the proposed HRES, ensuring the optimal energy balance between the different multiple energy sources and the load at each hour of operation. The result of the size optimization model showed that an LCOE for implementing an HRES in the community would be 0.48 USD/kWh in a full-battery-capacity scenario and 1.17 USD/kWh in a half-battery-capacity scenario. The result from this study is important for quick decision-making and effective feasibility studies on the optimal technoeconomic synopsis of implementing minigrids in rural communities.

**Keywords:** hybrid renewable energy system (HRES); particle swarm optimization (PSO); fuzzy logic control (FLC); energy management system (EMS); loss of power supply probability (LPSP); levelized cost of energy (LCOE); microgrid; Nigeria



**Citation:** Afolabi, T.; Farzaneh, H. Optimal Design and Operation of an Off-Grid Hybrid Renewable Energy System in Nigeria's Rural Residential Area, Using Fuzzy Logic and Optimization Techniques. *Sustainability* **2023**, *15*, 3862. <https://doi.org/10.3390/su15043862>

Academic Editor: Pablo García Triviño

Received: 20 January 2023  
Revised: 15 February 2023  
Accepted: 17 February 2023  
Published: 20 February 2023



**Copyright:** © 2023 by the authors. Licensee MDPI, Basel, Switzerland. This article is an open access article distributed under the terms and conditions of the Creative Commons Attribution (CC BY) license (<https://creativecommons.org/licenses/by/4.0/>).

## 1. Introduction

### 1.1. Background

Nigeria, the most populous country in Africa, has one of the lowest rates of electrification in the world [1]. About 43% of the Nigerian population, representing 85 million people, have no access to grid electricity [2]. Nigerian households connected to the grid have electricity only for about 7 h per day and experience more than 10 blackouts every week, and most people run diesel or gasoline generators for more than 4 h a day [3]. Those who receive electricity from the grid experience more than 17 h of blackout per day. Therefore, most households and businesses resort to self-electricity generation using alternative sources such as diesel or gasoline.

Nigeria's national grid is currently being managed by the following: the Nigeria Electricity Regulatory Commission (NERC), which is responsible for formulating policies and regulating the power sector, and the Power Holding Company of Nigeria (PHCN), which is accountable for coordinating the investments and operations of the power sector. This duo was created in 2005 after the National Electric Power Authority (NEPA) was decoupled when the Electric Power Sector Reform Act (EPSRA) was enacted for the privatization of the power sector [4]. PHCN is currently being grouped into three divisions, which include generation companies (GENCOs), a transmission company (TRACO), and 11 distribution companies (DISCOs). The GENCOs consists of more than 5) independent

power producers (IPPs), 10 national integrated power projects (NIPPs), and 6 privatized PHCNs, which include Afam, Egbin, Kainji, Sapele, Shiroro, and Ughelli Power Plc; the TRACO is the Transmission Company of Nigeria (TCN), and the 11 DISCOs include the Abuja Electricity Distribution Company, the Benin Electricity Distribution Company, the Ibadan Electricity Distribution Company, the Eko Electricity Distribution Company, the Enugu Electricity Distribution Company, the Ikeja Electricity Distribution Company, the Jos Electricity Distribution Company, the Kaduna Electricity Distribution Company, the Port Harcourt Electricity Distribution Company, the Kano Electricity Distribution Company, and the Yola Electricity Distribution Company [5]. The GENCOs are responsible for producing electricity, the TRACO is responsible for transmitting electricity from the GENCOs to the DISCOs, and the DISCOs are responsible for distributing electricity to the final consumers.

The present total installed capacity of the GENCOs is around 12.5 GW, out of which 5.4 GW is inaccessible and 3.3 GW is nonfunctional, leaving only around 3.9 GW of electricity for the GENCOs to functionally produce and dispatch to the TRACO; 0.3 GW is lost while transmitting to the DISCOs, leaving around 3.6 GW for the DISCOs to distribute to the final consumers; 0.5 GW is lost during distribution so only about 3.1 GW is distributed to the final consumers [6,7]. Figure 1 shows the Nigeria Power Sector energy flow in megawatts (MW). Nigeria's daily electricity need is approximately 8 GW to 17 GW, although estimating Nigerians' electricity need is complicated by the passive demand from unavailable electricity [1]. Given that the Nigerian population is over 200 million people [8] and the rule-of-thumb estimates of 1 GW per 1 million people [7], Nigeria will supply the electricity needed to support full industrialization only once the country can produce up to 200 GW of electricity. According to the World Bank, Nigeria's electricity consumption stands at 144.52 kWh per capita, compared with over 5500 kWh per capita in European countries [9].

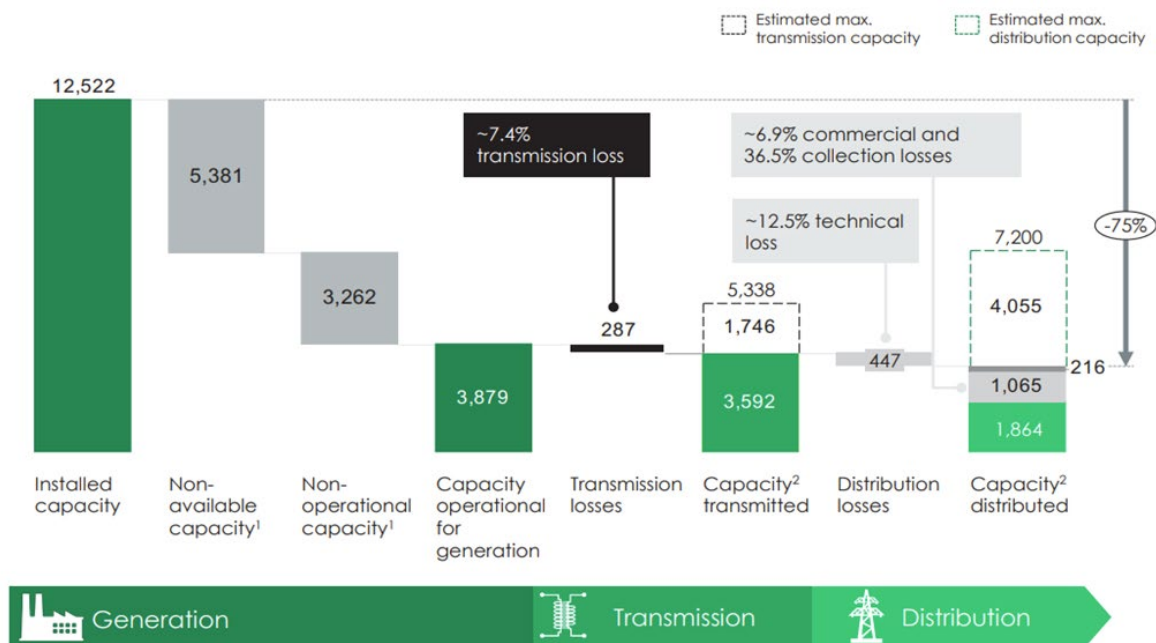


**Figure 1.** Nigeria Power Sector energy flow (adapted from [6]).

The above data show that Nigeria's current generation capacity is far below what the population demands. This imbalance between the electricity generated and the demand creates an epileptic and unreliable electricity situation in the country. Furthermore, the data show that only around 25% of the installed capacity reaches the final consumer; this is partially connected to the gas supply disturbances in that most electricity-producing plants are gas fueled. In fact, 85% of the total installed capacity is generated by gas-fueled thermal power plants, and the remaining 15% is generated by hydroelectric power plants [6].

Therefore, to meet Nigeria's electricity demand, generating energy by using fossil fuels is not advisable, owing to these technical challenges and the severe environmental and health impacts of using fossil fuels. It is, therefore, important to assess the renewable energy potential for electricity generation in Nigeria.

Renewable energy has become a panacea to energy problems worldwide because it is clean, environmentally friendly, and ultimately cheaper. Nigeria has a massive capacity for generating electricity from its numerous green energy resources, with a daily energy potential of 934 GWh from biomass, 120 GWh from solar, 84 GWh from hydro, and 44 GWh from wind [10]. Nigeria's photovoltaic power output potential (kWh/kWp) is shown in Figure 2, while the wind speed available in each Nigeria state is shown in the wind resource map of Nigeria in Figure 3.

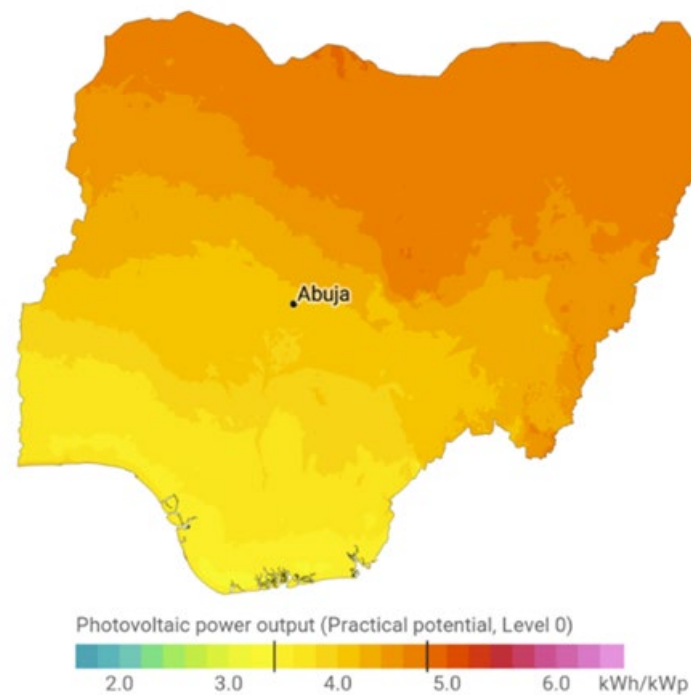


Figure 2. Nigeria photovoltaic power output potential [11].



Figure 3. Wind resource map of Nigeria [12].

Stears Data reported that even though there are many potential renewable energy solutions obtainable in Nigeria, solar energy is the best at providing electricity for off-grid areas in Nigeria because of its sufficiency, relatively low cost, and different strata available for different levels of consumers [1]. Additionally, electricity generated in off-grid regions is best consumed where they are generated. Dispatching the produced electricity to the national grid will cause only more losses and more uncertainty in transmission to the end users. Nigeria's transmission grid critically restricts the proportion of the produced electricity that reaches the final consumers. Outworn and ineffective equipment, a deficient framework, and insufficient investment in extending the grid have made accessing electricity through the grid ineffective in the long term [1]. It is thus essential to investigate how off-grid electricity can be positioned to supplement the void in the electricity supply. Shaaban and Petinrin pointed out that exploiting off-grid green energy potentials in Nigeria could reduce the persistent electricity crisis in the country [13]. The present paper, therefore, focuses on the techno-economic study of implementing an off-grid hybrid renewable energy system in Nigeria and proposes an EMS that would ensure the reliability of the HRES operation. It uses a community situated in the southwestern part of Nigeria as a case study.

This study is motivated by the proliferation of the adoption of renewable energy systems for generating electricity. This has been due to advocacy by governments and international organizations for the supply of renewable energy to remote regions that are off the grid and to reduce the world's environmental impact from greenhouse effects exacerbated by nonrenewable energy production and consumption. These developments have increased efforts to establish renewable energy plants in many nations to access more-sustainable energy and combat environmental degradation and climate change issues [14]. However, the usage of these renewable energy systems is usually in hybrid forms because the availability of all renewable energy sources is not dependable. A hybrid renewable energy system (HRES) integrates many renewable technologies and operates as an independent power system with higher reliability than a single renewable energy source [15]. Because renewable energy is sourced from the natural environment, it is dependent on weather conditions, which makes it difficult to design stable electricity systems that use renewable sources [16]. The two most important renewable energy sources for off-grid distributed energy systems, namely wind and photovoltaic (PV) sources, are affected by random fluctuations owing to their dependence on short-term weather and seasonal climate variations [17]. A hybrid renewable energy system (HRES) contains a microgrid or decentralized generation (DG) that consists of two or more renewable energy sources, such as solar PVs, wind turbines, fuel cells, and other renewable energy sources working together with other decentralized nonrenewable power generation units in a coordinated manner to meet the demand of a particular area [18]. Storage systems such as batteries and hydrogen fuel cells and emergency generation equipment such as a diesel generator are always included in the hybrid renewable energy systems to back them up against fluctuation and to ensure reliability. Energy-storage equipment stores excess energy, which is released when renewable energy is not available, thereby solving the fluctuation problems associated with renewable energy sources [19], while a diesel generator (DG) is added as an emergency power source to improve HRES reliability [20].

However, the addition of these different units to an energy supply system makes the system more complex in terms of both technological adaptability and economic sustainability. In addition, the operating characteristics and costs of HRES are much higher than those of standalone wind turbines or solar PV systems [21]. This, therefore, calls for designing a cost-effective HRES and an efficient energy management system (EMS) that ensures economic sustainability and technical adaptability for the hybrid system; such a system would ensure optimal operation cost and energy system reliability by reducing the system's LPSP.

## 1.2. Literature Review

Because of the various equipment involved in HRES, excessive sizing leads to exorbitant capital, and insufficient sizing leads to an unreliable system. The two situations are unwanted; therefore, optimal sizing is important when planning HRES. There have been numerous studies on sizing models for HRES, where each of them uses either economic indicators (such as net present value (NPV), levelized cost of electricity (LCOE), total annual cost (TAC), and cost of electricity (COE)), reliability indicators (such as deficiency of power supply probability (DPSP), loss of load probability (LOLP), and loss of power supply probability (LPSP)), environmental indicators (such as life-cycle emission (LCE), carbon footprint of energy (CFOE), life-cycle assessment (LCA)), or social indicators (such as social acceptance (SA), the job-creation index (JCI), and the Human Development Index (HDI)) as its objective indexes for evaluating the HRES's performance. Most studies have prioritized economic and/or reliability as objective indexes: 43.5% of the surveyed papers have prioritized economic indexes, and 37% have prioritized both economic and reliability indexes as objective indexes [22]. This means that over 80% of the surveyed publications on HRES sizing have prioritized economics and reliability indexes in evaluating their HRES's performance.

HRES sizing includes mostly conventional strategies (such as the analytical method, numerical method, iterative method, and probabilistic method), artificial intelligence (AI) techniques (such as the particle swarm optimization (PSO), cuckoo search algorithm (CSA), genetic algorithm (GA), ant colony optimization (ACO), artificial bee colony (ABC), and gray wolf optimization (GWO)), hybrid methods (such as GA-ABC, simulated annealing-tabulated search (SA-TS), and divide and conquer-remote electrical tilt (DP-RET)), and computer software (such as the hybrid optimization model for electric renewables (HOMER), general algebraic modeling system (GAMS), transient system simulation tool (TRNSYS), hybrid optimization by genetic algorithm (HOGA), LINGO, and HYBRIDs) [22]. Analogous to conventional strategies, AI methods deal with intricate and nonlinear problems while dealing with incomplete data and fluctuating wind and solar energy problems [23]. Among the AI strategies, PSO and GA have higher use cases. GA and PSO constitute more than 50% of the use cases of all AI strategies [22]. Although GA is used more than PSO, PSO is appreciated for its ease of implementation, high accuracy, simple computation, fast convergence, absence of crossover, and lack of mutation operations present in GA [23,24].

Many HRES optimization studies have used PSO to optimize the power generated by HRES to meet the electrical needs of a typical home and minimize LCOE [25]. Yoshida and Farzaneh designed an optimal standalone microgrid system consisting of the wind, a PV, a battery, and a diesel generator on the basis of the PSO method to find the optimal system configuration by using the lowest-cost-perspective approach [26]. Mohammed et al. developed a PSO model to optimize the power generated by an HRES, which consists of a wind turbine, a tidal turbine, a solar PV, and batteries [27]. The system was designed to serve and minimize the energy cost of a standalone community in Bretagne, France. Naoto and Farzaneh utilized the PSO algorithm to realize the optimal configuration of an HRES to minimize the total cost of an HRES in an off-grid mode and maximize the total profit gained in a grid-tied mode while meeting the load demand of a typical residential household in Fukuoka, Japan [28].

Furthermore, there have been several studies on developing an energy management system (EMS) to ensure energy balance for an HRES. Currently, most of the EMS-related research on HRES has focused on distributed energy systems in microgrids and electric vehicles [29]. EMS strategies can be categorized into intelligence-based controls, such as wavelet neural networks (WNNs), machine learning, and multi-objective optimization methods; rule-based controls, such as the logic threshold and fuzzy logic control (FLC) methods; or optimal-based controls, such as instantaneous optimization and global optimization [29]. Of these methods, fuzzy logic control is considered important because its rules are easy to implement and do not involve complex mathematical modeling [29]. Abdullahi and Majed have shown the necessity of strengthening an HRES by having at

least two kinds of energy-storage systems and two kinds of renewable sources for system stability, and they designed an FLC for the energy management of HRES that has multiple types of storage [30]. However, the designed FLC cannot be applied to a more complex system involving a larger distribution network, as in the case of microgrids.

In a study comparing the technoeconomic analysis of solar home systems (SHSs) and microgrids to determine the best choice for rural electrification, Chaurey and Kandpal found that a microgrid is a more economical option for providing power to an off-grid community with more than 500 densely populated households [31]. The technoeconomic analysis of a microgrid, investigated by Borhanazad, through the design of a standalone off-grid hybrid PV/wind/diesel/battery system for a rural community in Malaysia showed that having 56–61% of solar energy inclusion is important to achieve an optimal and economically feasible hybrid system [32]. To minimize the power demand of buildings in Japan, Tatsuya et al. used a fuzzy logic controller to design a grid-tied hybrid solar/wind/hydrogen system with a maximum power point tracker (MPPT) and obtained a 2% excess power generation from the designed HRES [33]. Berrazouane proposed a cuckoo-search-algorithm-tuned FLC to operate an autonomous hybrid power system and discovered that the optimized FLC could reduce the LPSP, LCOE, and excess energy of the systems [34]. Table 1 summarizes the recent studies on the modeling of the HRES.

**Table 1.** Summary of literature survey on HRES.

Country	Research Goal	System Components	Objective Function	Optimization Method	Impact Category	Ref.
Japan	To design an optimal standalone microgrid for powering a residential area.	PV/wind/battery/DG	Total cost	PSO	Economic	[26]
France	To optimize the power generated by a hybrid renewable energy system	Wind turbine/tidal turbine/PV module/battery	Total net present cost	PSO	Economic	[27]
Australia	To control the power flow of an HRES with multiple renewable energy sources and multiple energy-storage systems	PV/wind/fuel cell/battery	EMS control	Fuzzy logic	Reliability	[30]
India	To make a technoeconomic comparison between an SHS and a microgrid	SHS/PV/wind/battery/DG	Annualized life-cycle costs (ALCCs)	HOMER	Economic	[31]
Malaysia	To investigate the technoeconomic analysis of an optimal standalone HRES in remote areas	PV/wind/battery/DG	COE LPSP	PSO	Economic, reliability	[32]
Japan	To reduce the load demand of buildings on an HRES	Grid-tied hybrid solar/wind/hydrogen	LCOE	Fuzzy logic	Economic	[33]
Algeria	To develop an optimal FLC for the operation of a standalone HRES that is based on a CSA	PV/battery/DG	LPSP, excess energy, LEC	Fuzzy logic	Economic, reliability	[34]

### 1.3. Research Gap and Research Contribution

Optimal sizing and control are two aspects of the same HRES. A system that is optimally sized but not optimally controlled will be inefficient. Optimal sizing ensures the minimal implementation cost and energy affordability, while optimal control ensures the optimal operation cost and energy availability. The literature survey showed that most

of the research studies have focused only on system sizing or energy control. However, the size, cost, control, and reliability of HRESs are all interdependent; an effective energy management system needs to be integrated with an appropriate sizing method. This research aims to develop an optimal sizing model that finds the lowest-cost configuration of the HRES, which is then integrated into an EMS model that ensures optimal energy scheduling during HRES operation in an off-grid community. The integration of the two systems will produce a combined model that ensures energy reliability at the optimal cost. The study uses PSO to find the equipment sizing that provides the best cost at optimal reliability and uses a fuzzy logic controller to design an EMS that every time ensures an energy balance between the energy demand and the energy supply during the HRES operation.

The rest of this paper is organized as follows: Section 2 introduces the size optimization model, the structure of the HRES, and the mathematical modeling of the constituent components of the HRES. Section 3 presents the design of an optimal fuzzy-logic-controlled energy management system. Section 4 shows the characteristics of the case-study community, the renewable energy resource data, the load data, the economic data, and the technical parameters of the equipment. Simulation results are presented and discussed in Section 5. Finally, the research objectives are achieved in Section 6, the concluding section.

## 2. Size Optimization Model

### 2.1. System Structure

Figure 4 shows the typical structure of the considered HRES. The system contains two renewable energy sources, solar photovoltaic modules, and a wind turbine. The battery is included as a backup power source, while the diesel generator serves as an emergency supply. An inverter is included that converts direct current to alternating current and vice versa. The consumer load is the energy demand of the community. The inverter is assumed to contain an energy management system that controls the power flow between the load demand and the different energy sources.

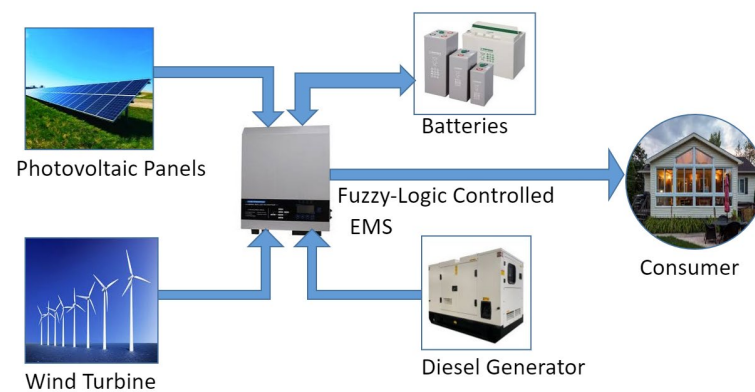


**Figure 4.** Hybrid renewable energy system structure.

The mathematical modeling of each component is explained in the following section.

### 2.2. Solar PV Model

Solar PV output power is influenced by factors such as solar irradiance, the yearly season, the surrounding temperature, the type of PV module, and the inclination angle. The solar panel output power  $P_{PV}$  is determined by a simplified simulation model and is given by following the equations [27]:

$$P_{PV} = N_{PV} \times \eta_{PV} \times A_m \times G_t \quad (1)$$

$$\eta_{PV} = \eta_{ref} \times \eta_{pc} \left[ 1 - \beta (T_c - T_{cref}) \right] \quad (2)$$

$$T_c = T_a + \left( \frac{NOCT - 20}{800} \right) \times G_t \quad (3)$$

where  $T_{a,NOCT} = 20$  °C and  $G_{t,NOCT} = \frac{800 \text{ W}}{\text{m}^2}$  are the wind speed of 1 m/s;  $N_{PV}$  is the number of PV panels;  $\eta_{PV}$  is the panel efficiency;  $A_m$  is the total area of the panel module;  $G_t$  is the incident global irradiance ( $\text{W}/\text{m}^2$ );  $T_a$  is the surrounding temperature; and  $NOCT$  is the normal PV working temperature (°C).

### 2.3. Wind Turbine Model

The power output of a wind turbine is determined by the regional wind speed and wind turbine characteristics. This study uses the following equations to determine the output power of a wind turbine [26]:

$$P_w(V) = \begin{cases} \frac{P_r(V - V_{CIN})}{V_{rat} - V_{CIN}} \cdot V_{CIN} & V_{CIN} \leq V \leq V_{rat} \\ P_r \cdot V_{rat} & V_{rat} \leq V \leq V_{CO} \\ 0 & V \leq V_{CIN} \text{ and } V \geq V_{CO} \end{cases} \quad (4)$$

$$V = V_{ref} \left( \frac{H}{H_{ref}} \right)^\alpha \quad (5)$$

where  $H_{ref}$  (m) is the reference height;  $V_{ref}$  (m/s) is the reference height's wind speed;  $\alpha$  refers to the exponent;  $H$  (m) is the height of the wind turbine;  $V$  is the wind speed at  $H$  (m);  $V_{rat}$  (m/s) is the rated wind speed of the wind turbine;  $P_r$  (kW) is the constant power;  $V_{CIN}$  (m/s) is the cut-in speed; and  $V_{CO}$  (m/s) is the cut-out speed.

### 2.4. Battery Model

A battery stores electrical energy in chemical form. Energy stored in the battery is used to power the load when renewable energy is not sufficient. The battery capacity can be estimated by the following equation [2]:

$$C_B = \frac{E_L \cdot S_D}{V_B \cdot DOD_{max} T_{cf} \cdot \mu_B} \quad (6)$$

where  $V_B$  is the battery working voltage;  $E_L$  is the load in Wh;  $T_{cf}$  is the temperature correction factor;  $S_D$  is the number of autonomy days;  $DOD_{max}$  is the depth of discharge; and  $\mu_B$  is the efficiency.

Additionally, the battery SOC is defined as the available capacity divided by the rated capacity of the battery in ampere hours (Ahr). This is mathematically expressed below [32]:

$$SOC = \frac{\text{Available Capacity (Ahr)}}{\text{Rated Capacity (Ahr)}} \times 100 \quad (7)$$

$$SOC(t) = SOC(t-1) \cdot (1 - \sigma) + \left[ E_{Gen(t)} - \frac{E_L(t)}{\mu_{inv}} \right] \mu_B \quad (8)$$

$$SOC(t) = SOC(t-1) \cdot (1 - \sigma) + \left[ \frac{E_L(t)}{\mu_{inv}} = E_{Gen(t)} \right] \mu_B \quad (9)$$

$$SOC = 1 - DOD \quad (10)$$

where  $E_L$  is the load,  $\sigma$  is the self-discharge rate an hour, and  $E_{Gen}$  is the energy generated. Equation (8) is used for the battery charging, while Equation (9) is used for the battery discharging. The battery optimally operates between the allowable discharge limit, denoted as  $SOC_{low}$ , and the allowable maximum charge limit, denoted as  $SOC_{max}$ .

2.5. Power-Flow Strategy

For the optimal sizing of the HRES using the PSO, the power-flow needs to be balanced such that renewable energy is optimally utilized while ensuring that energy is always available to power the load. The HRES considered in this study comprises the PV, a wind turbine, a battery, a DG, and the load. The power management for the PSO ensures that a balance between the energy supplied and the energy demanded. At every hourly time step, the PSO program compares the renewable energy (solar and wind) with the load and then decides whether to charge the battery, discharge the battery, or start the diesel generator, depending on the conditions. When the energy supplied by renewable energy (RE) is enough to power the load, the excess energy is used to charge the battery. When the RE is not enough to power the load and the battery SOC is greater than the lowest SOC, energy is taken from the battery to power the load. When the RE is insufficient to power the load and the battery SOC is lower than the lowest SOC, the diesel generator is switched on to power the load, and the diesel generator’s excess energy is used to charge the battery. The flowchart of the power-flow strategy is shown in Figure 5.

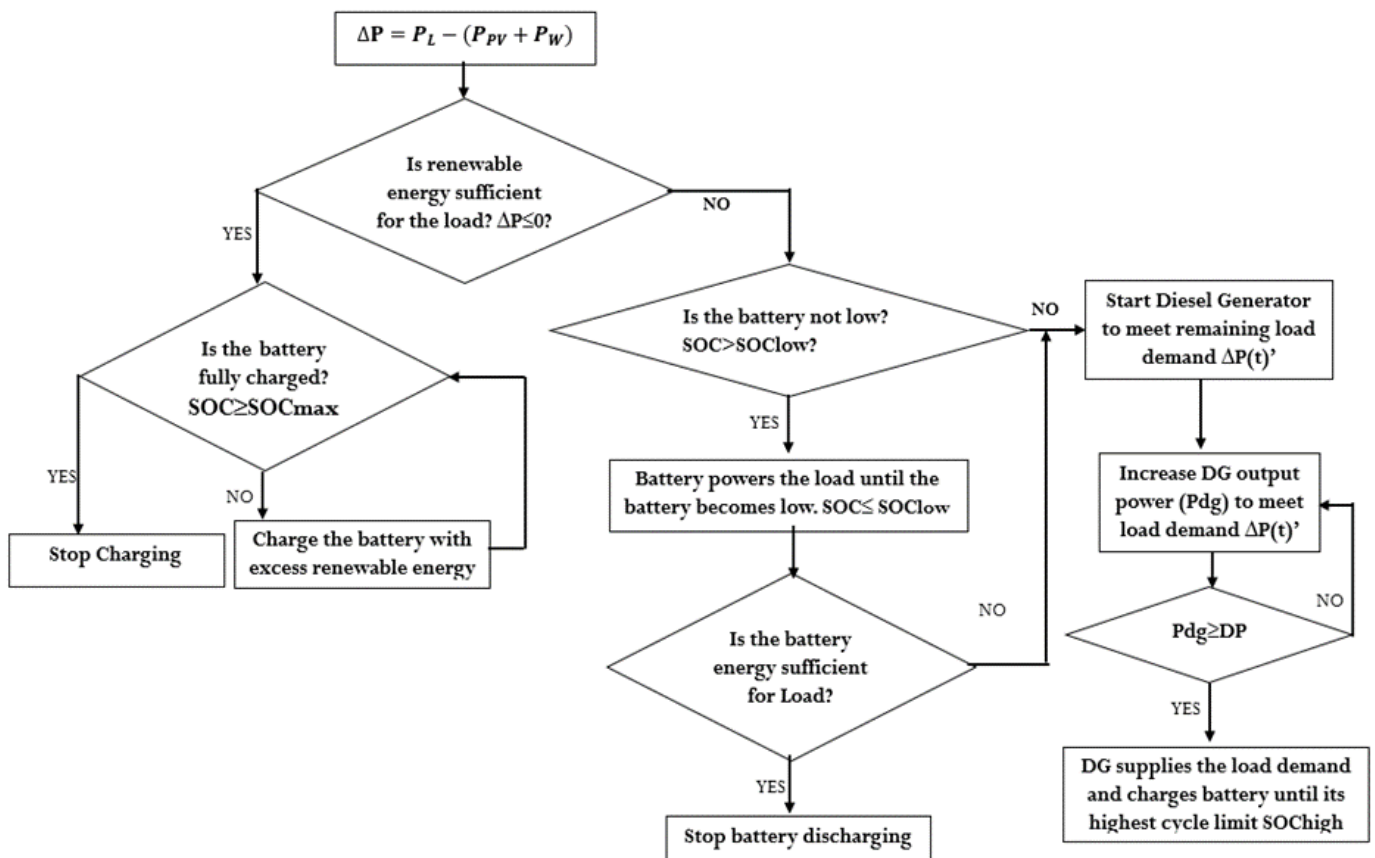


Figure 5. Power-flow strategies for the PSO optimization.

2.6. Operating Cost of an HRES

The battery replacement cost and the diesel generator running cost constitute the main operating costs of the considered HRES because other sources have only capital costs, with little to no maintenance costs.

### 2.6.1. Replacement Cost of Batteries

The cost of replacing batteries majorly contributes to the overall operating cost of an HRES. Battery replacement depends on the battery usage cycle  $N_T$ , which in turn is dependent on the depth of discharge (DOD). The operating cost of the battery ( $C_{Bat}$ ) in (USD/kWh) is given as follows [21]:

$$C_{Bat} = \frac{\sum_{j=0}^{N_T} C_j}{\sum_{j=0}^{N_T} |\Delta P_{batj}|} \quad (11)$$

where  $N_T$  refers to the battery cycle during the operating period,  $\Delta P_{batj}$  is the battery power output during operating hour  $j$ , and  $C_j$  is the life cost of the battery.  $C_j$  is given as follows:

$$C_j = \frac{C_{initial-bat}}{N_C} \quad (12)$$

where  $C_{initial-bat}$  refers to the battery purchase price and  $N_C$  is the maximum number of battery cycles.

### 2.6.2. Operation Cost of the Diesel Generator

In an HRES, a generator provides the energy needed to power the load at a critical time when renewable energy and battery energy are not enough. A generator needs to be run between 70% and 89% of its rated capacity for optimal efficiency [35]. The fuel consumption of a diesel generator can be mathematically expressed as follows [36]:

$$D_f(t) = \alpha_D P_{DG}(t) + \beta_D \times P_{Dr} \quad (13)$$

where  $D_f(t)$  in (Liter/hour) refers to the fuel consumption,  $P_{DG}(t)$  in (kW) refers to the DG power generation,  $P_{Dr}$  in (kW) refers to the rated power, and  $\alpha_D$  and  $\beta_D$  refer to the fuel consumption curve coefficients, which are taken as 0.2461 L/kWh and 0.08415 L/kWh, respectively [36]. The fuel cost ( $C_g$ ) is given as follows:

$$C_g = \frac{D_f(t)C_f}{P_{DG}} = C_f \left( \alpha_D + \frac{\beta_D \times P_{Dr}}{P_{DG}} \right) \quad (14)$$

where  $C_f$  is the diesel price.

The DG depreciation cost is given as follows:

$$C_{DW} = \frac{\frac{M_T}{20,000} C_{initialDG}}{\sum_{t=0}^{M_T} P_{DG}(t)} \quad (15)$$

where  $M_T$  refers to the DG's operating hours and  $C_{initialDG}$  refers to the DG cost of purchase. The operating cost of the diesel generator ( $C_{DG}$ ) is given as follows:

$$C_{DG} = C_g + C_{DW} \quad (16)$$

### 2.7. Particle Swarm Optimization (PSO) Model

In 1995, Kennedy and Eberhart proposed the particle swarm optimization algorithm [37]. PSO is a stochastic optimization algorithm based on the population of particles. It has been successfully used in many applications, such as face detection, voice recognition, and neural network training, because it computes in parallel with fast computing speed. PSO mimics the characteristics of a flock of birds, called a "swarm", with a single possible bird called a "particle", which is the solution. The fitness value for each solution is evaluated for every particle by using the fitness function. A velocity vector is also evaluated for each particle. Every solution is updated for each particle in the search space. Each solution is compared over several iterations with the particle's previous and neighbor's positions

to determine the optimal value [38]. To reach the optimal point, each particle updates its position in its search space according to its previous experience and those of its neighbors over iterations. The movement of the particle depends on its present velocity and every element  $j$  of the velocity vector of the  $k$ th particle is expressed as follows:

$$V_i^{(k+1)} = \omega \times V_i^{(k)} + C_1 \times rand_1(\cdot) \times P_{best,i} - X_i^{(k)} + C_2 \times rand_2(\cdot) \times (G_{best} - X_i^{(k)}) \quad (17)$$

$$X_i^{(k+1)} = X_i^{(k)} + V_i^{(k+1)} \quad (18)$$

where  $X_i^{(k+1)}$  refers to the new position of the  $i$ th particle;  $V_i^{(k+1)}$  refers to the new velocity vector of the  $i$ th particle;  $rand_1(\cdot)$  and  $rand_2(\cdot)$  are random numbers, each within  $[0, 1]$ ;  $C_1$  and  $C_2$  refer to the learning factors;  $\omega$  is the momentum weight factor;  $P_{best,i}$  is the prior best experience of the  $i$ th particle that is recorded; and  $G_{best}$  refers to the best particle of the entire population.

The PSO algorithm is used to determine the optimal sizes of the HRES equipment by minimizing the cost (LCOE) function:

$$LCOE \left( \frac{USD}{kWh} \right) = \frac{\text{Annualized Cost (USD)}}{\text{Annual Energy Supplied (kWh)}} \quad (19)$$

$$= \frac{NPC \text{ (USD)}}{P_{load} \text{ (kW)} \left( 8760 \frac{\text{h}}{\text{year}} \right)} \times CRF \quad (20)$$

$$CRF = \frac{i(i+1)^n}{(1+i)^n - 1} \quad (21)$$

where  $n$  is the project life (24 years),  $i$  is the prevailing interest rate,  $NPC$  is the net present cost and comprises all capital costs, and  $P_{load}$  (kW) includes all energy supplied in one year. The cost function is subjected to technical and reliability constraints. The reliability constraint (LPSP) is defined as follows:

$$LPSP = \frac{\sum P_{load} - P_{pv} - P_{wind} - P_{battery} - P_{DG}}{\sum P_{load}} \quad (22)$$

where  $P_{pv}$  is the PV power,  $P_{wind}$  is the wind power,  $P_{DG}$  is the diesel generator power, and  $P_{battery}$  is the usable energy of the battery. The LPSP is to be less than 0.2%. Kashefi et al. stated that an LPSP of less than 1% is acceptable for off-grid electricity supplies as compared with an LPSP of less than 0.01%, which is accepted in developed countries [39].

The renewable energy resource data include solar irradiation data, wind data, and temperature data, and the equipment characteristics and load consumption data of the community are used to determine the optimum value for the equipment. The load is preferably powered by using renewable energy (RE), and power is drawn from the battery only when renewable energy is insufficient. The system uses a diesel generator for emergency supply when the RE is unavailable and when the battery energy is inadequate for the demand. A flowchart of the PSO algorithm is shown in Figure 6.

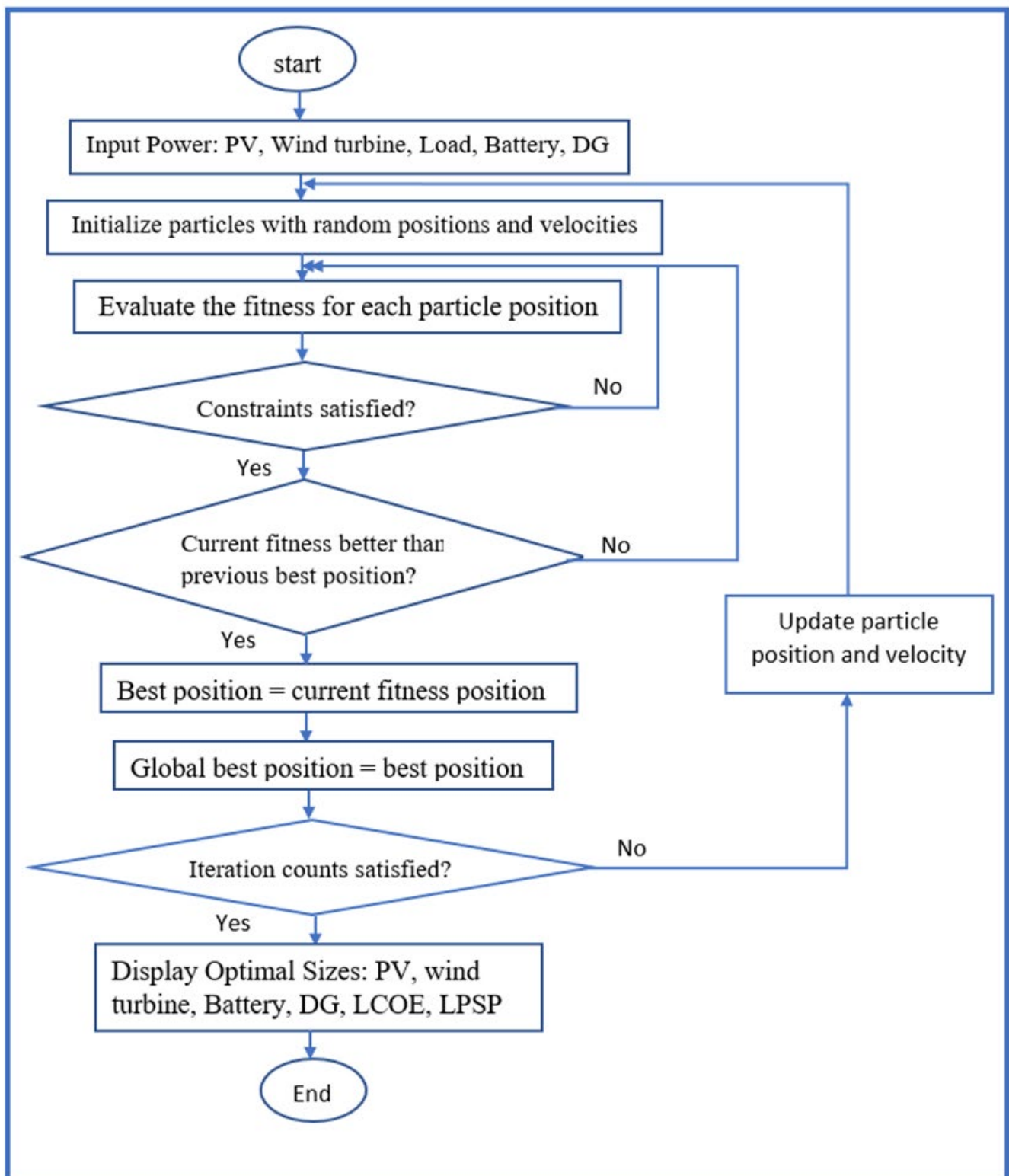
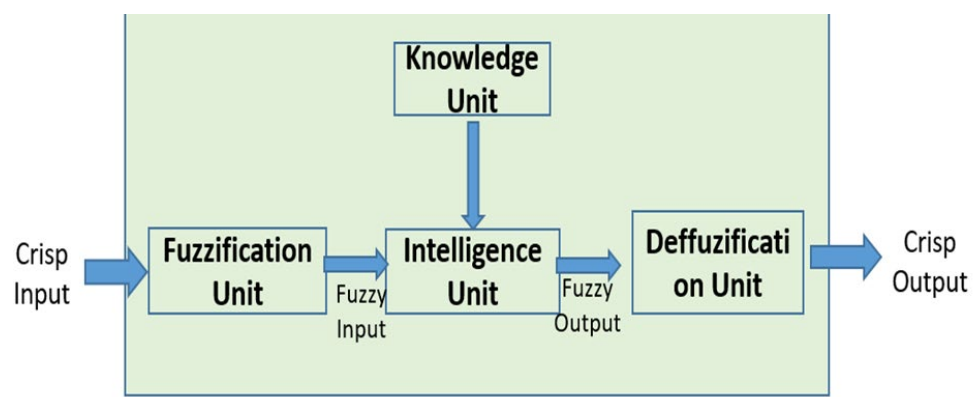


Figure 6. Flowchart of the particle swarm optimization (PSO) algorithm.

### 3. Optimal Energy Management System Using a Fuzzy Logic Controller

A fuzzy logic control is established on multivalued logic that allows for using common principles and expert knowledge for control rules [40]. Its control method is like human reasoning methods. L.A. Zadeh pioneered the idea of fuzzy logic in 1965 [41], and it has since been developed and adapted for different systems to provide effective and efficient

control in many applications. Zadeh defined a fuzzy set as a collection of objects with varying grades of membership identified by a membership function that allocates a scale of membership ranging from zero to one for every object [41]. Fuzzy logic control involves the application of fuzzy sets and theories in control processes. The fuzzy logic control method uses range-to-range or range-to-point strategies—unlike the classical control method, which uses point-to-point control. The fuzzy system (Figure 7) comprises four units: a fuzzification unit, a knowledge unit, an intelligence unit, and a defuzzification unit. Inputs are converted into fuzzy inputs by assigning the associated membership functions to the imprecise inputs at the fuzzification unit. The intelligence and knowledge units work on the fuzzy inputs and infer the proper results by considering the rules to produce a fuzzy output that is converted back to crisp output at the defuzzification unit [30,42]. The fuzzy logic controller is efficiently employed for energy management control thanks to its simple and effective feature adaptability to the nonlinearity of HRES energy supply and demand [34].



**Figure 7.** Fuzzy logic control structure.

### 3.1. Design of the Energy Management System

The main function of the energy management system in an HRES is to control the energy flow from each energy source to the load. An optimal energy management system will ensure an energy balance between the demand and the supply and guarantee the maximum utilization of the available renewable energy. At every point during the HRES operation, the EMS works to ensure that the power flow satisfies the energy balance between the components, as shown in the equation below:

$$P_{pv}(t) + P_w(t) + P_{batt\_discharge}(t) + P_{DG}(t) = P_l(t) + P_{batt\_charge}(t) \quad (23)$$

In the EMS considered, the PV power ( $P_{pv}$ ) and wind power ( $P_w$ ) are renewable energy (RE) power. The load is preferably powered by using renewable energy (RE), and power is drawn from the battery only when renewable energy is insufficient. The system considers using a diesel generator for emergency supply when the RE is unavailable and when the energy available on the battery is inadequate for the demand or when the battery has depleted to its minimum allowable state of charge (SOC). The differential power ( $\Delta P$ ) is the power difference between the load power ( $P_L$ ) and renewable energy (RE):

$$\Delta P = P_L(t) - (P_{pv}(t) + P_w(t)) \quad (24)$$

The battery state of charge (SOC) for the FLC is modeled by using the SOC equation presented by [21]:

$$SOC(t) = \frac{P_{batt}(t-1) + C_{batt}[P_{RE}(t) - P_L(t)] + \{P_{DG}(t) - (1 - C_{batt})[P_L(t) - P_{RE}(t)]\}}{P_{batt}} \quad (25)$$

where,  $P_{batt}(t-1)$  is the remaining energy on the battery in the last hour;  $C_{batt}[P_{RE}(t) - P_L(t)]$  refers to the current RE charging power or load discharging power;  $\{P_{DG}(t) - (1 - C_{batt})[P_L(t) - P_{RE}(t)]\}$  indicates the current generator charging power; and  $P_{batt}$  is the battery-rated capacity. If the renewable energy power (RE) is sufficient for the load ( $\Delta P \leq 0$ ) and if the battery is fully charged ( $SOC \geq SOC_{max}$ ), then the battery stops charging. If the renewable energy power  $\Delta P$  is sufficient for the load ( $\Delta P \leq 0$ ) but the battery is not fully charged ( $SOC < SOC_{max}$ ), then the excess renewable energy charges the battery until the battery is charged to the maximum ( $SOC_{max}$ ). If the renewable energy power  $\Delta P$  is insufficient for the load ( $\Delta P > 0$ ) and if the battery is charged ( $SOC > SOC_{low}$ ), then the battery discharges to power the load until the battery becomes low ( $SOC \leq SOC_{low}$ ); if the battery energy is sufficient for the load, then the battery stops discharging. If the battery energy is insufficient for the load or if the battery is low ( $SOC \leq SOC_{low}$ ), then the diesel generator starts to meet the remaining load demand ( $\Delta P'$ ); the DG output power adjusts to meet the remaining load demand until the diesel generator output power is sufficient ( $P_{dg} \geq \Delta P'$ ). The DG supplies the load demand and charges the battery until the battery is fully charged ( $SOC \geq SOC_{max}$ ). Figure 8 shows the flowchart of the energy management system considered in this study.

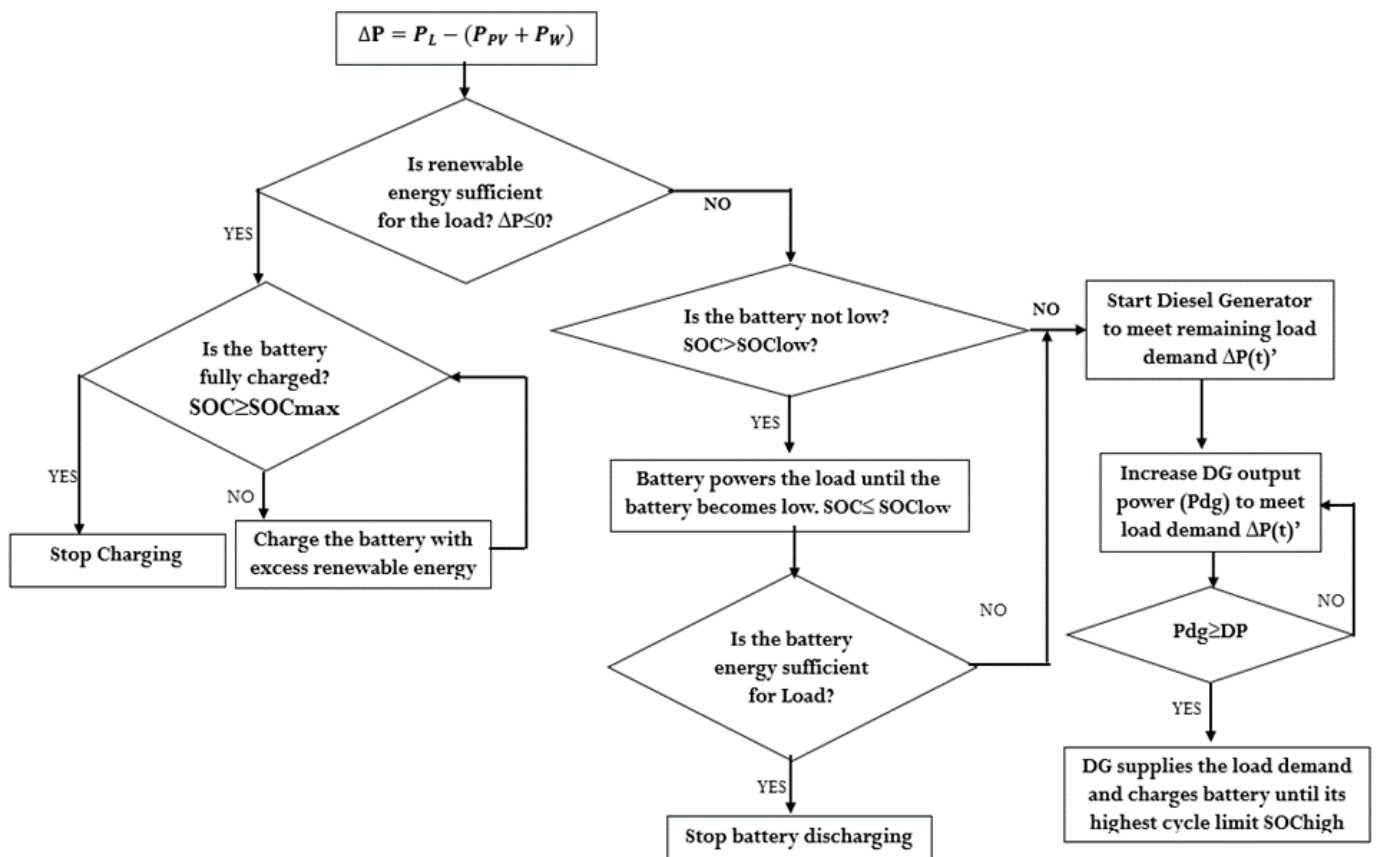


Figure 8. Flowchart of the energy allocation processes.

For efficient and optimal power control, the fuzzy logic controller is designed to schedule among the energy sources and establish the energy balance of both the supply and the demand sides. The solar irradiation data, the wind data, the equipment sizing obtained from the PSO optimization model (discussed in Section 2), and the load consumption data are considered to analyze the performance and effectiveness of the fuzzy logic controller. The fuzzy-logic-controlled energy management system (FLC-EMS) was designed in MATLAB Simulink IDE, v.2022b. The hybrid renewable energy system was first designed by using the optimal sizes of the equipment obtained from the optimal sizing

model, the power demand, the solar irradiance, and the wind speed data of the community. Figure 9 shows the interconnection between the designed HRES and the designed FLC energy management system. The solar power, wind power, load power, and battery power signals from the HRES are used as inputs into the FLC energy management system. This study uses two FLC controllers, denoted as FLC1 and FLC2. Figure 10 shows the HRES simulation diagram.

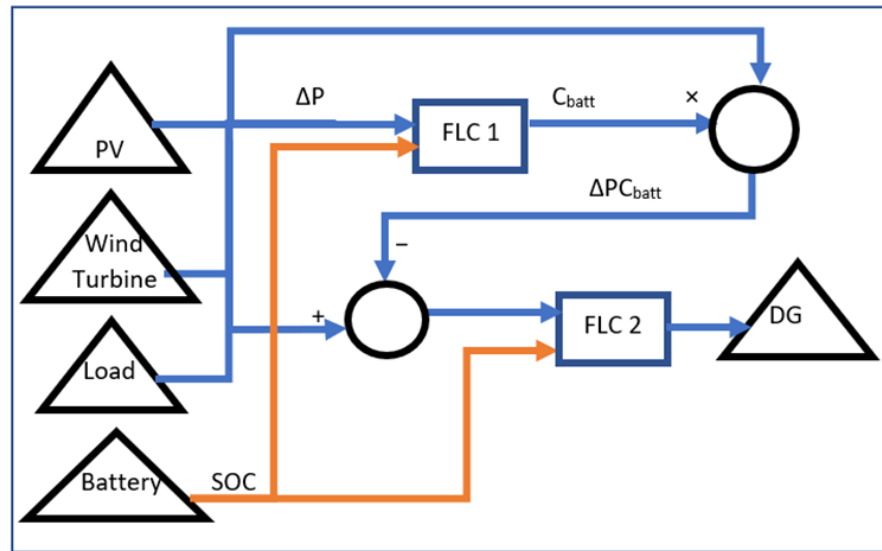


Figure 9. The signal flow of the fuzzy logic controllers.

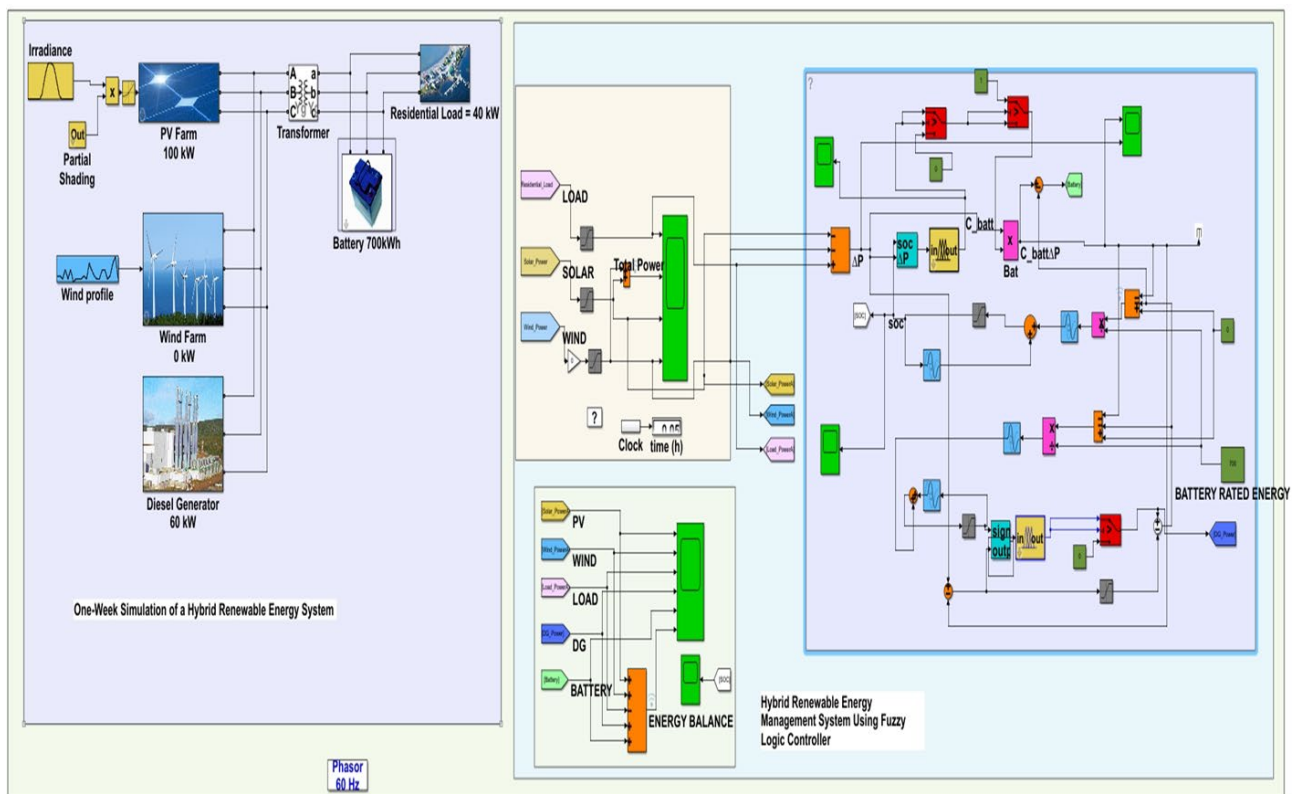


Figure 10. The designed HRES and FLC in MATLAB Simulink IDE.

The fuzzy logic controllers operate on the basis of the strategies discussed in Section 3.1. Tables 2 and 3 show the control rules to be implemented by FLC1 and FLC2, respectively.

**Table 2.** Fuzzy logic rules for FLC1.

$\Delta P(t)/SOC$	Multiplier ( $C_{batt}$ )						
	ML	L	SL	S	SH	H	MH
NH	MH	MH	MH	MH	MH	MH	ML
NS	MH	MH	MH	MH	MH	MH	ML
NL	MH	MH	MH	MH	MH	MH	ML
PL	ML	ML	ML	ML	MH	MH	MH
PS	ML	ML	ML	ML	MH	MH	MH
PH	ML	ML	ML	ML	MH	MH	MH

**Table 3.** Fuzzy logic rules for FLC2.

$\Delta P(t)/SOC$	PDG(t)						
	ML	L	SL	S	SH	H	MH
NH	VL	VL	VL	VL	VL	VL	VL
NL	VL	VL	VL	VL	VL	VL	VL
NS	VL	VL	VL	VL	VL	VL	VL
PL	VL	VL	VL	VL	VL	VL	VL
PS	S	S	S	VL	VL	VL	VL
PH	H	H	MH	MH	VL	VL	VL
PMH	VH	VH	VH	MH	VL	VL	VL
PVH	VH	VH	VH	MH	VL	VL	VL
PMVH	VH	VH	VH	MH	VL	VL	VL

These rules are based on the operator's/expert's knowledge. For membership functions, "V" represents "very", "L" represents "low", "H" represents "high", "S" represents "standard", "M" represents "much", "P" represents "positive", and "N" represents "negative". Battery SOC, input 1 to FLC1, has a universe of discourse running from 0 to 1 and has seven variables. The differential power ( $\Delta P$ ), input 2 to FLC1, has its universe of discourse running from  $-80$  to  $60$  kW and has six variables. The two inputs produce a total of 42 fuzzy logic rules. The battery multiplier constant,  $C_{batt}$ , which is the output of FLC1, has its universe of discourse run from 0 to 1. The  $C_{batt}$  membership function also has seven variables. The membership function for each variable is plotted as shown in Figure 11. Battery SOC ( $t-1$ ), which is input 1 to FLC2, has its universe of discourse run from 0 to 1 and has seven variables, and the excess power,  $\Delta P$ , which is input 2 to FLC2, has its universe of discourse run from  $-80$  to  $40$  kW and has nine variables. The two variables give rise to a total of 63 fuzzy logic rules. The diesel generator output power,  $P_{DG}$ , which is the output of FLC2, has its universe of discourse run from 0 to  $50$  kW and has eight variables. The membership functions of the variables are plotted as shown in Figure 12.

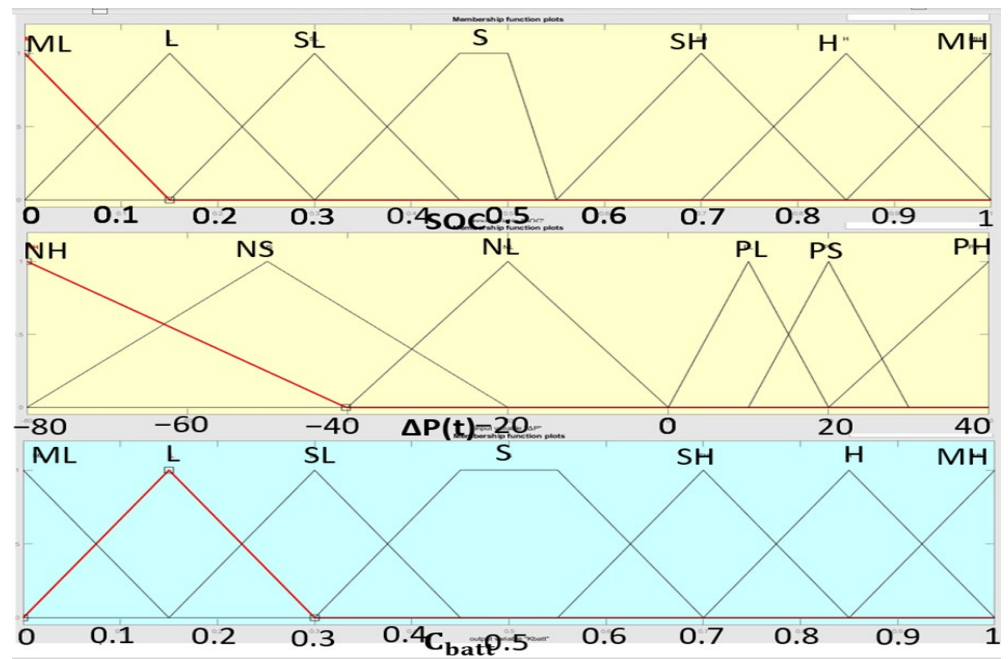


Figure 11. The membership functions of the FLC1 variables.

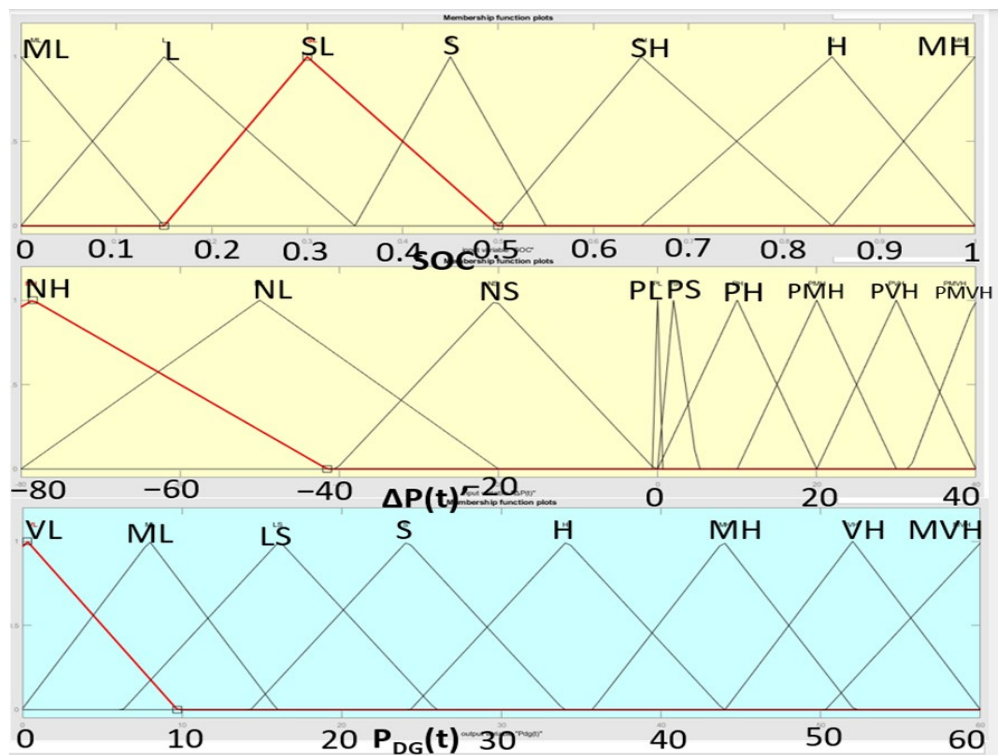
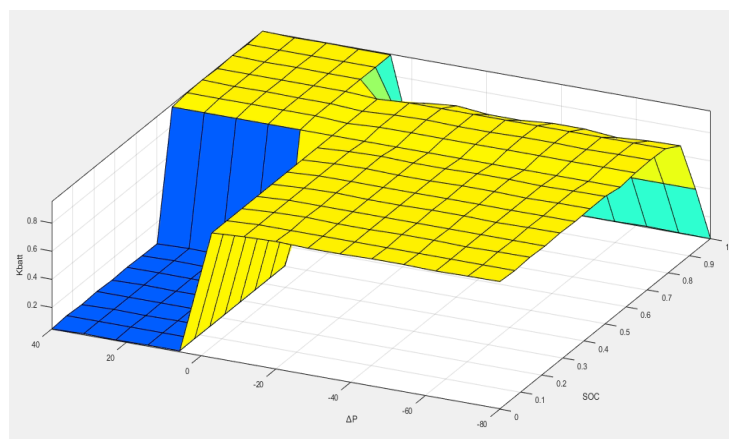


Figure 12. The membership functions of the FLC2 variables.

### 3.2. Formation of FLC1 Rules

The fuzzy logic rules for FLC1 are shown in Table 3. The power difference ( $\Delta P$ ) between the current power demand and the current renewable power is the first input into FLC1, while the battery state of charge (SOC) is the second input. The controller uses the value of  $\Delta P$  and SOC at each time to determine whether to charge the battery or discharge the battery. The correction power factor  $C_{batt}$  is the output of FLC1 that determines how much energy is used to charge the battery or is discharged from the battery. Figure 13 shows a three-dimensional view of the output of the FLC1 controller.



**Figure 13.** Three-dimensional plot of FLC1 rules.

### 3.3. Formation of FLC2 Rules

The fuzzy logic rules for FLC2 are shown in Table 4. FLC2 decides when to switch on the diesel generator to power the excess load. The power gap ( $\Delta P'$ ), which is the net load minus the battery discharging power and the previous state of charge (SOC( $t-1$ )), are the inputs to FLC2. The controller uses values of ( $\Delta P'$ ) and SOC ( $t-1$ ) to decide whether to start the DG. When the SOC is low and there is excess load, the controller starts the DG. When the SOC is low and when there is excess RE, the controller will not start the DG. When the SOC is high and when there is excess load, the controller will not start the DG. The controller will start the DG when there is excess RE and when SOC is high. The DG power ( $P_{DG}$ ), the FLC2 output, supplies the load, and the extra energy from the DG is used to charge the battery. Figure 14 shows a three-dimensional view of the output of the FLC2 controller.

**Table 4.** Investment cost analysis.

Equipment	Initial Cost (USD/kW)	Lifetime (Years)	Efficiency
PV (including PV cable and PV mounting accessories)	704.63	24	
Wind turbine and wind-turbine-installation accessories	1619.74	24	
Battery (including battery cable and battery rack)	188.17	16	0.85
Diesel generator (DG accessories and ATS)	156.13	24,000 h	
Inverter and accessories	645.69	24	0.92
PV controller (including accessories)	102.09	24	0.95

Table 4. Cont.

Equipment	Initial Cost (USD/kW)	Lifetime (Years)	Efficiency
Wind turbine controller and accessories	102.09	24	0.95
Construction (including powerhouse, fencing, and PV array foundation)	357.32		
Development and installation	320.33		
Distribution and metering	1063.70		
Fuel costs	USD 1.57 per liter		
Interest rates	11.5		
Project lifetime		24	
Operation and maintenance costs	20% of the initial cost		

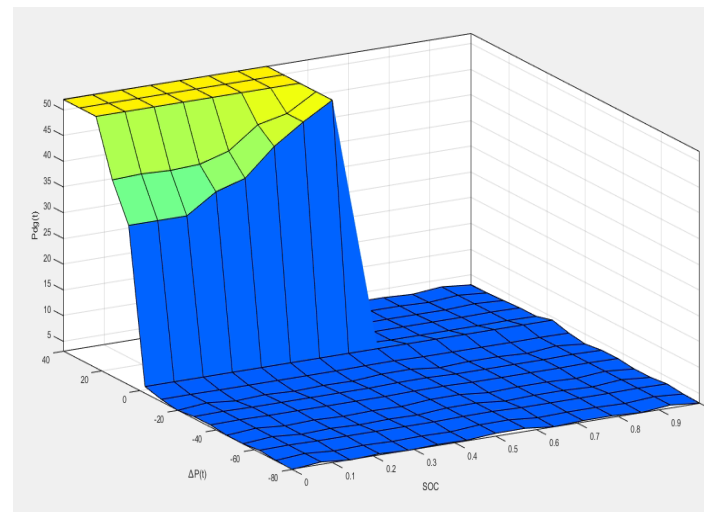
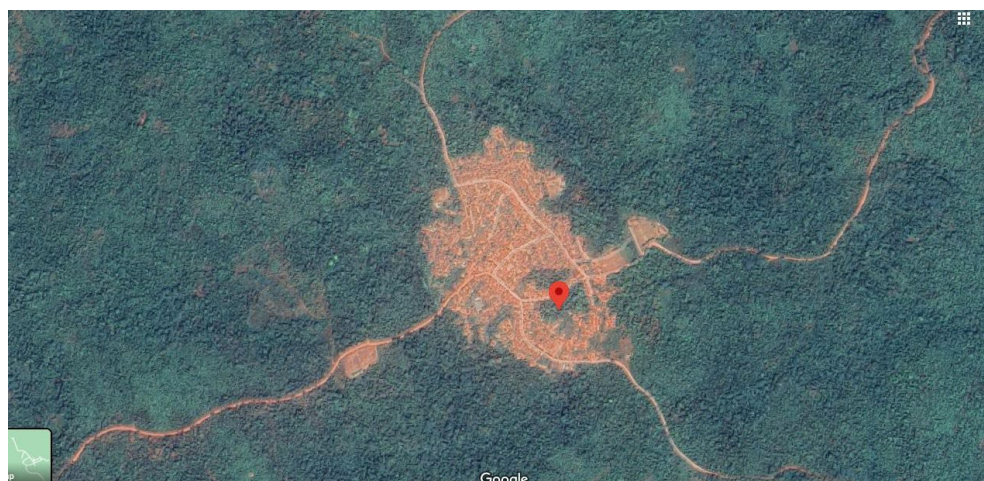


Figure 14. Three-dimensional plot of FLC2 rules.

## 4. Data and Case Study

### 4.1. Case Study

The case study is an isolated off-grid rural community called Olooji, in the Ijebu-East Local Government Area of Ogun state, Nigeria. Olooji is an agrarian community located on latitude  $06^{\circ}53.329'$  N and longitude  $04^{\circ}27.342'$  E. Olooji falls within the tropical rain forest, which is typical of the regions in the southern part of Nigeria. It has two seasons: the dry season (October–March) and the wet season (April–September). The number of households in Olooji is about 600, with an average size of 11 people per household, comprising mostly children and women. Olooji is estimated to have a population of up to 7000 people. The community is about 60 km and around two hours' drive on an untarred muddy road from the nearest national grid, in the Orita J4 Express community. Olooji heads over 10 nearby villages and runs on a self-employed agrarian economy, where mainly female merchants sell agricultural produce, food, and clothing in roadside shops. Olooji is currently being electrified by a solar minigrid system constructed and operated by ACOB Lighting Technology Limited, a private solar minigrid developer in Abuja, Nigeria. Figure 15 shows a satellite view of the Olooji community.



**Figure 15.** Satellite view of the Olooji community (courtesy of Google Earth).

#### 4.1.1. Load Profile

The hourly load demand of the Olooji community was collected for 24 h from the daily records by the minigrid operator via their SMA platform. Figure 16 shows the typical daily load profile of the Olooji community as obtained from the developer's load monitoring platform. From the daily load profile, the hourly average consumption in the community was 23.3 kWh, and the annual energy consumption in the community was estimated to be 202 MWh.

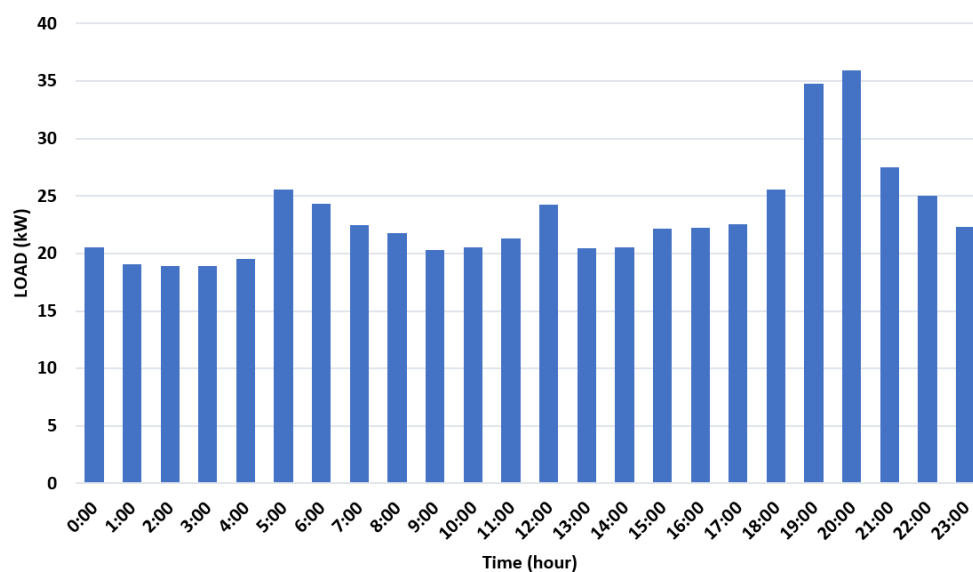


**Figure 16.** Typical daily load profile of Olooji community.

#### 4.1.2. Solar Irradiance, Wind Speed, and Temperature Data

Olooji solar irradiance, wind speed, and temperature data for 1 year, running from 1 January 2016 to 31 December 2016 (Figures 17–19), were collected from the National Aeronautic Space Agency (NASA) website [43].

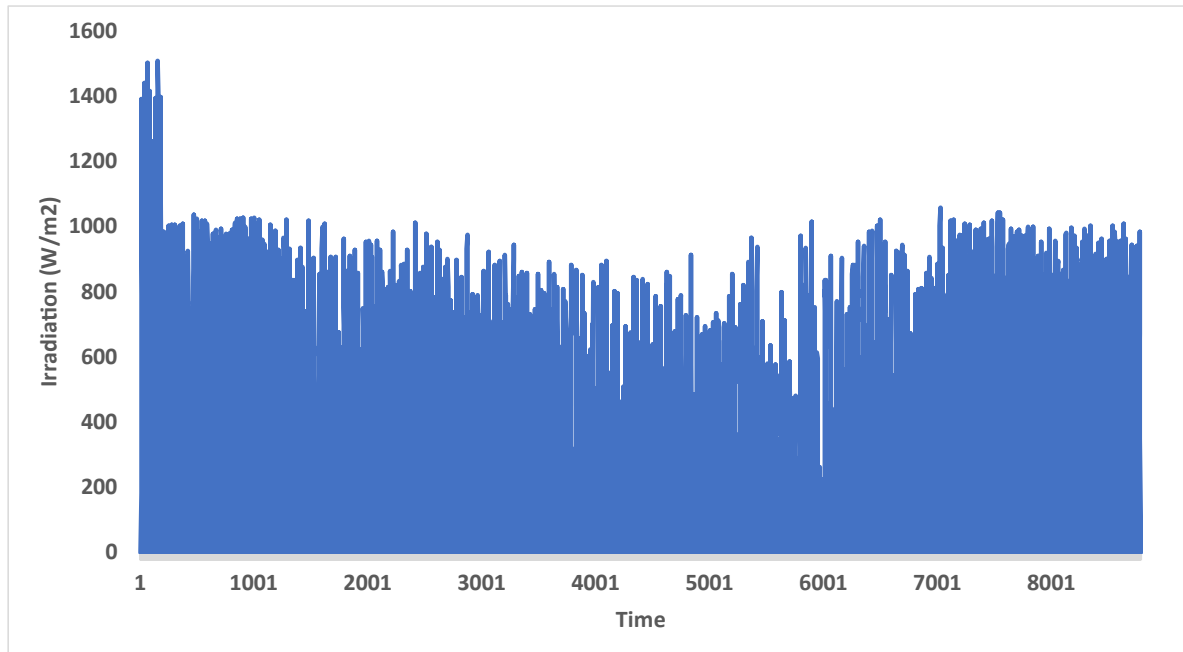


Figure 17. Olooji irradiation data for 1 year.

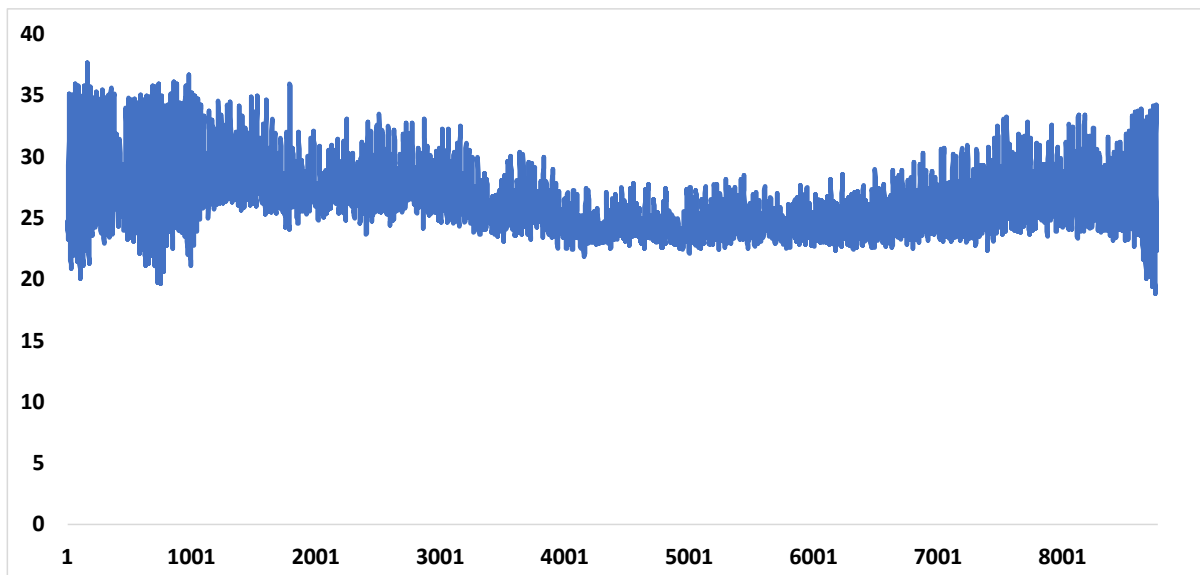


Figure 18. Olooji temperature data for 1 year.

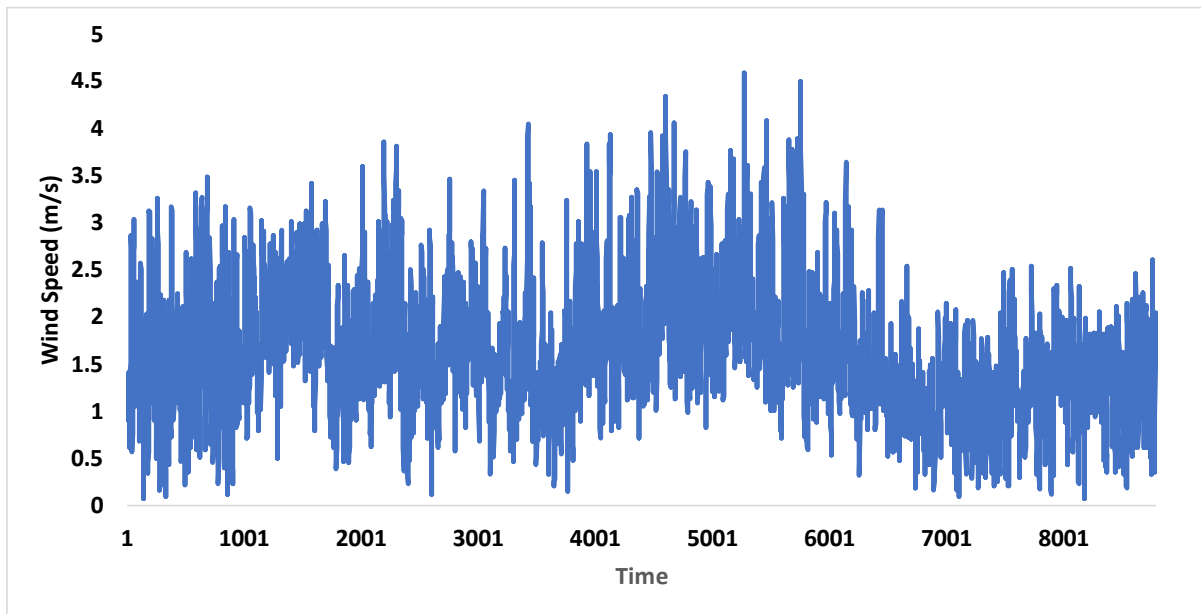


Figure 19. Olooji wind speed data for 1 year.

#### 4.2. Battery Life Cycle

The battery life cycle was determined by using the graph that shows the service life in cycles versus the depth of discharge (*DOD*) in the data sheet from the Hoppecke battery's original equipment manufacturer (OEM), shown in Figure 20 [44]. Figure 21 represents the cost of operation plotted under different state of charge (*SOC*) ranges [21]; the best operating cost, when DG is used in HRES, is at the lower bound *SOC* of 55% and the upper bound *SOC* of 75%. For this research, the lower bound *SOC* considered is 55%, which corresponds to a *DOD* of 45%, and the upper bound *SOC* considered is 80%, which corresponds to a *DOD* of 20%. The battery was assumed to run a daily cycle. This means that the battery is being charged to the maximum *SOC* and fully discharged to the minimum *SOC* every day (every 24 h).

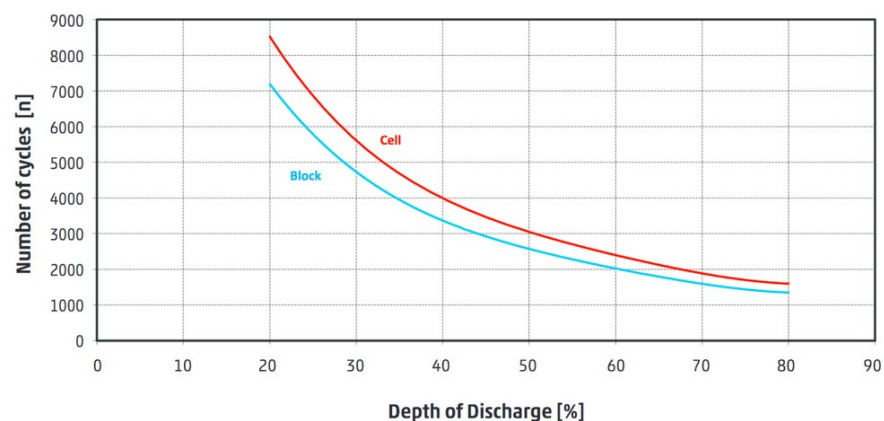


Figure 20. Number of cycles versus depth of discharge (adapted from [44]).

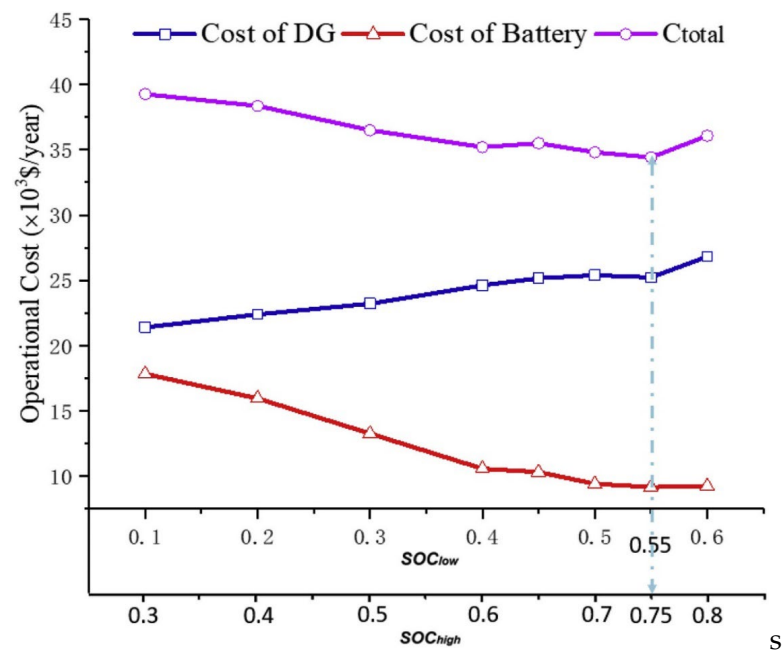


Figure 21. Cost of operation under different SOC ranges (adapted from [21]).

#### 4.3. Investment Cost Analysis

The investment costs of the HRES components are given in Table 4. The values were derived primarily from the financial budget for implementing a solar minigrid site from ACOB Lighting Technology Limited, the minigrid operator. The costs of the equipment were collected from the original equipment manufacturers (OEMs) and by surfing the OEM websites. The initial costs are considered as follows:

- PV panels and accessories, including the PV cable and mounting accessories.
- Battery and battery accessories, including battery cable and battery rack.
- Diesel generator (DG) and DG accessories.
- Inverter and inverter accessories.
- Distribution costs, including erecting the electric poles, aluminum conductor steel-reinforced (ACSR) cable, recline cable, and stay wires.
- Metering, including the meter, protective circuit breaker (PCB), and data concentrator unit (DCU) to monitor consumer consumption.
- Development and installation costs, including the cost of the land acquisition, cost of land clearing and preparation, cost of feasibility studies, environmental impact assessment (EIA) cost, technical design cost, Nigerian Electricity Management Service Agency (NEMSA) permit cost, Nigeria Electricity Regulatory Commission (NERC) license cost, Rural Electrification Agency (REA) license cost, and cost of acquiring the land title/certificate of occupancy (C of O) by the state government.
- Wind turbines and accessories costs were collected from ATO, a manufacturer of wind turbines.
- Fuel cost was estimated at USD 1.57/L, the equivalent of NGN 700/L, the prevailing diesel price in Nigeria as of June 2022. The interest rate of 11.5% was Nigeria's prevailing interest rate as of June 2022.

## 5. Results and Discussion

### 5.1. Size Optimization Results

The developed PSO codes were run for January (dry season) and August (rainy season), representing the two seasons in Nigeria. The codes were run in the MATLAB environment at several iterations to evaluate the LCOE while keeping the LPSP at a maximum of 0.2%. Two scenarios were considered. In the first scenario, the boundary conditions used were expanded to allow the algorithm to choose the equipment values without restrictions. In the second scenario, the boundary conditions were restricted to limit the battery size to those realistically and economically obtainable. The two scenarios are shown in Table 5.

**Table 5.** Basic assumptions used in two scenarios.

Equipment	1st Scenario		2nd Scenario	
	Minimum Capacity	Maximum Capacity	Minimum Capacity	Maximum Capacity
PV	0 kW	150 kW	0 kW	100 kW
Wind Turbine	0 kW	100 kW	0 kW	100 kW
Battery	0 kWh	2000 kWh	0 kWh	700 kWh
Generator	0 kW	100 kW	0 kW	100 kW

Table 6 shows the result of the developed PSO codes that were run for 100 iterations of the two scenarios.

**Table 6.** Result of the PSO optimization algorithm.

Equipment Capacity	1st Scenario	2nd Scenario
PV	130 kW	100 kW
Wind Turbine	0 kW	0 kW
Battery	1370 kWh	700 kWh
Generator	0 kW	25 kW
LPSP	0.20%	0.05%
LCOE	0.48 USD/kWh	1.17 USD/kWh

The LCOE values for scenarios 1 and 2 were estimated at 0.48 USD/kWh (LPSP = 0.20%) and 1.17 USD/kWh (LPSP = 0.05%), respectively. For the two scenarios, wind power was not used. This could be explained by the fact that the wind speed in the case-study community is deficient. Hence, using the wind turbine to meet the extra energy required would be more expensive. The second scenario required a diesel generator that was not needed in the first scenario. This raised the LCOE higher, by more than 150%, because of the excessive cost of fuel required to run the diesel generator. In both scenarios, the LPSP of 0.2% and 0.05% were within acceptable limits, ensuring adequate and reliable electricity supply to the community.

The effect of the two seasons (dry and wet seasons) in Nigeria can be compared by using the combined graphs of the simulation output. Figure 22a shows the power distribution of all energy sources using 1 week of data in January (dry season) in the first scenario, while Figure 22b shows the power distribution of all energy sources using 1 week of data in August (wet season) in the first scenario. Figure 23a shows the distribution of all energy sources using 1 week of data in January (dry season) in the second scenario, while Figure 23b shows the distribution of all energy sources using 1 week of data in August (wet season) in the second scenario. Figure 24a,b shows the LCOE values for the first and second scenarios, respectively.

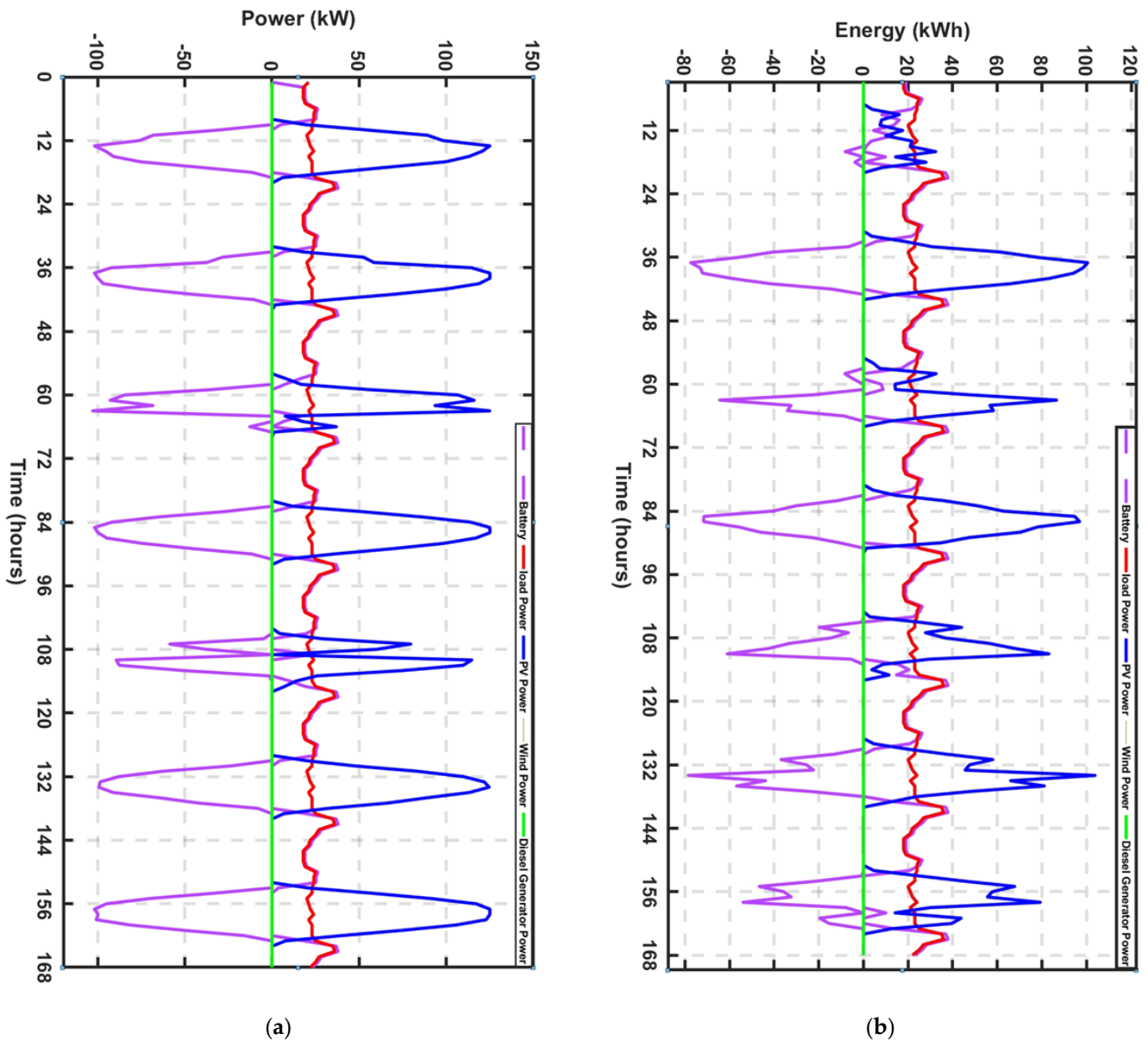


Figure 22. Power distribution in the first scenario: (a) January (b) August.

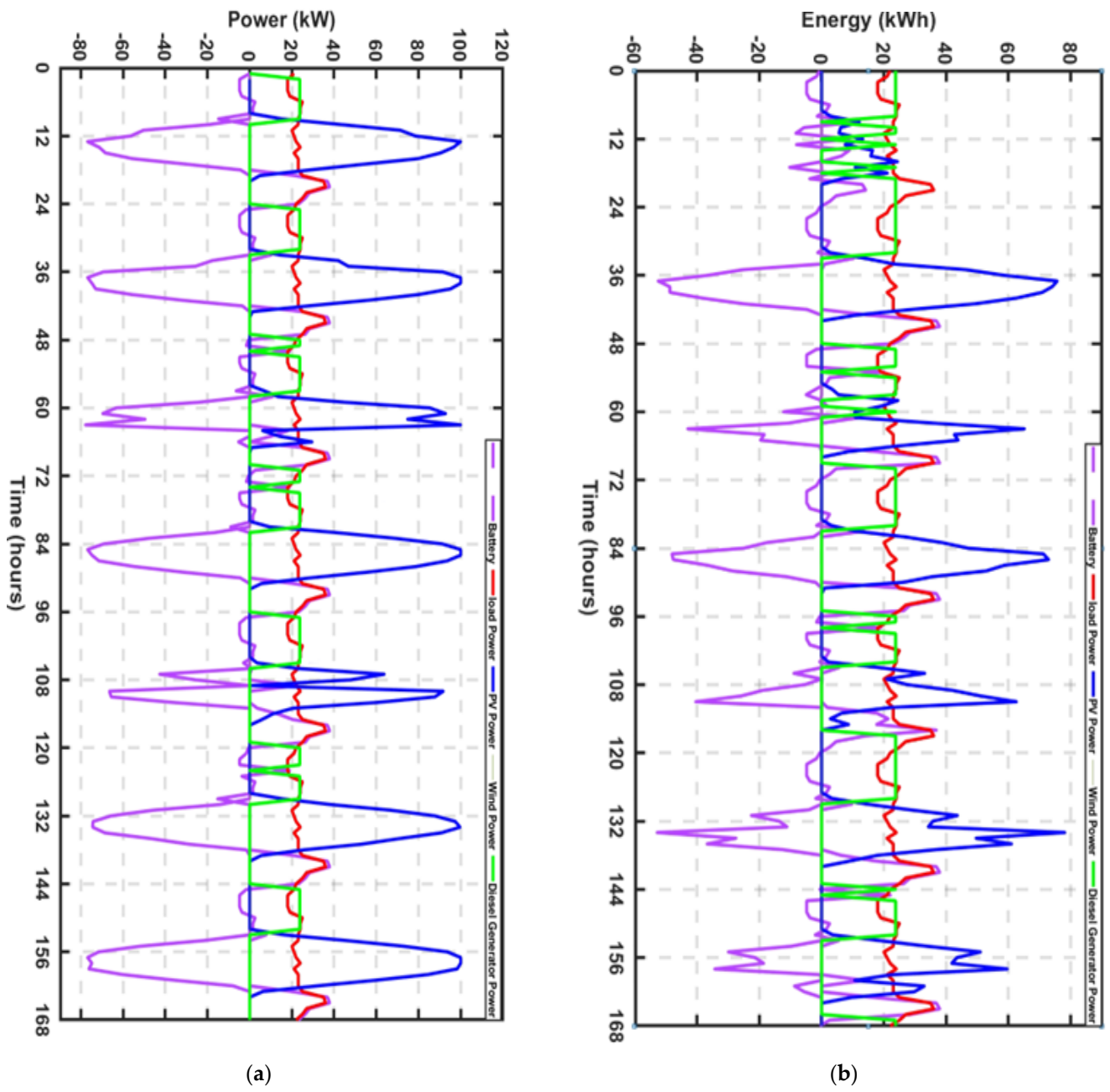


Figure 23. Power distribution in the second scenario: (a) January (b) August.

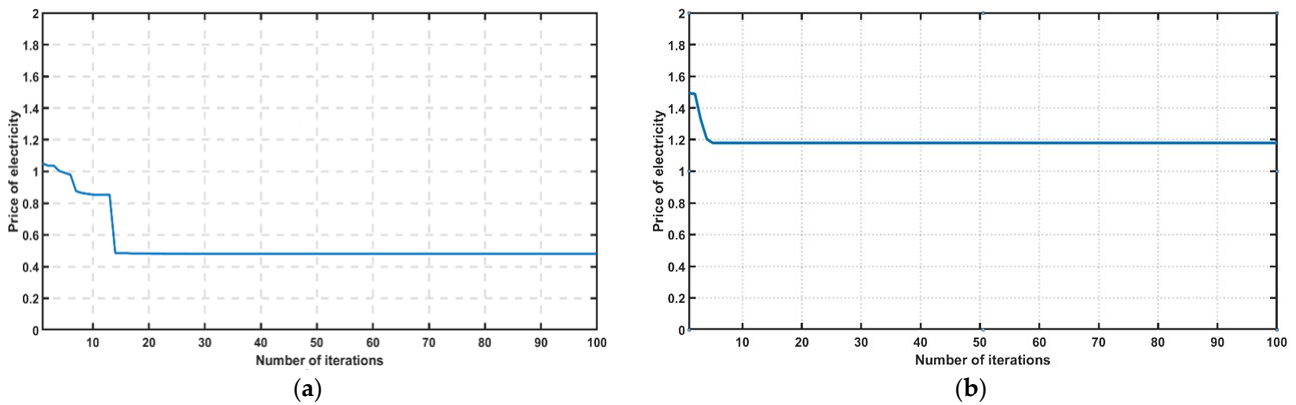


Figure 24. LCOE values for 100 iterations: (a) first scenario (b) second scenario.

It can be seen from the power distribution of each month that the solar power generation during the wet season (August) was low compared with that of the dry season (January). However, in the first scenario, a diesel generator was not used for both the dry and the rainy seasons. In the second scenario, the diesel generator was used for the two seasons and more hours during the wet season in August than during the dry season in January. The diesel generator was used during most of the nights in August to compensate for the deficiency in the renewable energy generated.

The monthly energy contributed by each energy source for the first scenario is shown in Figure 25; solar energy is the only energy source available for scenario 1. The monthly energy contributed by each energy source for the second scenario is shown in Figure 26. For both scenarios, the seasonal effects can be seen in the amount of energy generated from the PV. More solar energy was produced during the dry season (October–March), and less diesel energy was used. On the other hand, less solar energy was produced during the rainy season (April–September), and more diesel energy was used. For both scenarios, the total annual energy generated equaled the total annual energy demanded plus the total annual lost energy factored into the efficiency of the equipment.

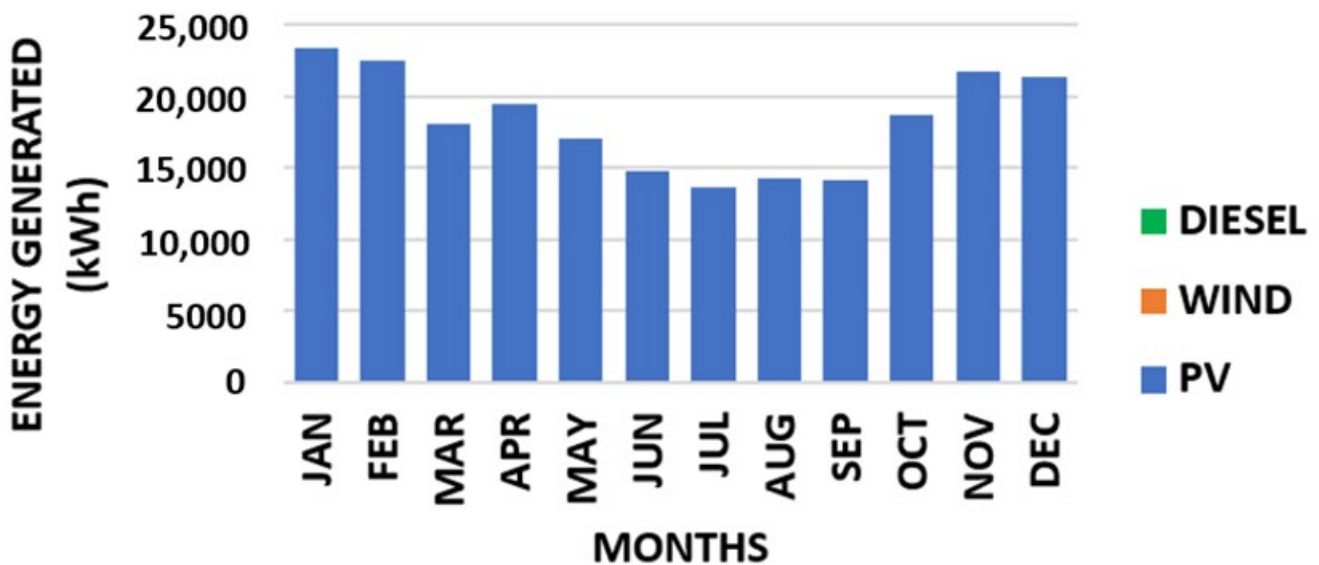


Figure 25. Monthly energy contribution by each source: first scenario.

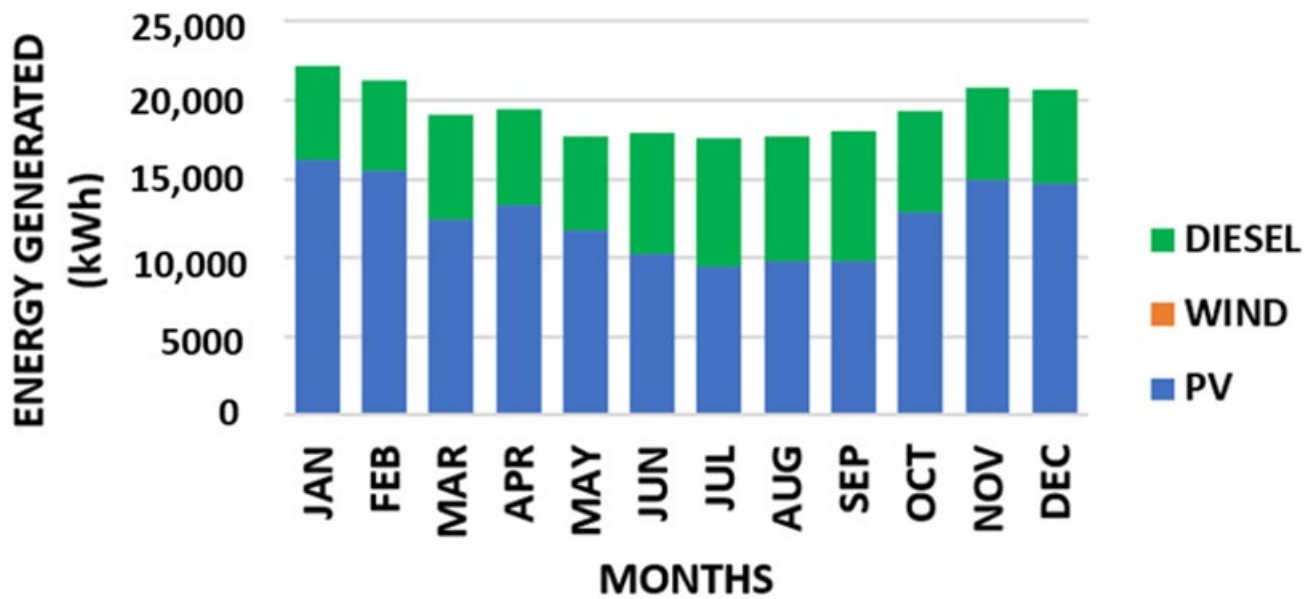


Figure 26. Monthly energy contribution by each source: second scenario.

### 5.2. Comparing This Paper's LCOE Result with LCOE Values from Other Studies

The LCOE result from this study was compared with LCOE results from other studies on HRES in other countries, as shown in Table 7. The system configuration of the compared studies includes the solar PV, the wind turbine, the battery, and the diesel generator. Result from this study is within the range of results from other studies. However, variation in the cost of equipment, cost of operation, cost of transportation, road networks, security, government incentives, and regulation are among the factors responsible for the variation in the LCOE values among the different countries.

Table 7. Comparing this paper's LCOE to LCOE values of other studies.

System	Country	LCOE (USD/kWh)	Ref.
This study (PV/battery)	Nigeria	0.48	This study
This study (PV/battery/diesel)	Nigeria	1.17	This study
Hybrid wind/solar PV/diesel/battery,	India	0.76	[45]
Solar PV/wind/diesel	Indonesia	1.06	[46]
PV/wind/battery/diesel	Japan	0.88	[26]
Typical off-grid microgrid in Pacific Island: PV/diesel	Pacific Island	1–1.7	[26]
Solar PV/diesel/wind/battery	South Africa	0.41	[47]
Solar PV/diesel	Ecuador	0.46	[48]

### 5.3. Fuzzy Logic Controller Results

The performance indicators for the fuzzy-logic-controlled EMS are the SOC of the battery and the energy balance of the HRES. By using the FLC-EMS, the SOC is expected to be kept within a certain range to ensure battery longevity. The energy balance of the HRES for each time unit measures the effectiveness of the EMS. The energy balance is the summation of all energy sources minus the load, and it is expected to be zero if the supply meets the demand at each time. Figure 27a,b show the combined diagrams of all energy sources, for January (a) and August (b), respectively. These figures show that the energy

balance (blue line) is equal to zero for each hour, indicating that the fuzzy logic controller effectively ensures energy balance.

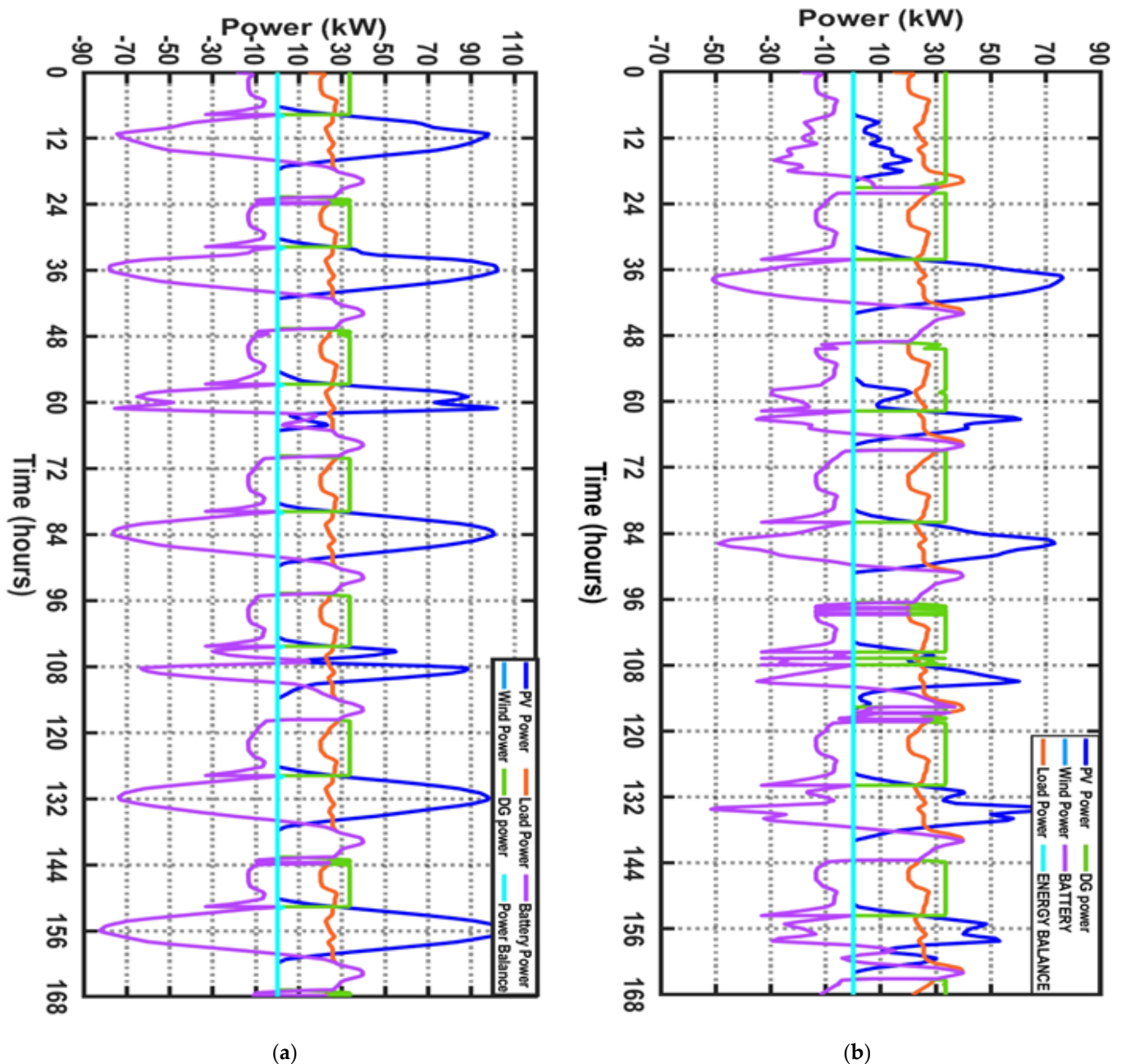


**Figure 27.** Power distribution of all energy sources for 1 week in the second scenario: (a) January and (b) August.

Figure 27a shows the combined diagram of all energy sources and the demand for the dry season (January), while Figure 27b is the combined diagram of all energy sources for the wet season (August). The FLC-EMS enabled the HRES to reliably and satisfy operate the load at each hour of operation. It can be seen that when solar energy was available, it was used to meet the load demand, and excess solar energy was used to charge the battery. When there was no more solar energy, the energy on the battery was discharged to meet the load demand. When the energy on the battery depleted to its minimum state of charge, the diesel generator was switched on to meet the load demand. The diesel generator was immediately switched off; there was energy from the PV the following day.

Furthermore, by comparing the two seasons, it can be seen that more solar energy was generated during the dry season than during the wet season, and by the same comparison, more DG energy was used during the wet and dry seasons. In either case, there was no output power from the wind turbine, because the wind turbine was not considered in this FLC-EMS, because the wind turbine sizing from the PSO algorithm was zero. The generator sizing used in the FLC (35 kW) was higher than the sizing from the PSO (25 kW). This was to provide operating tolerance and stability for the DG. The extra energy from the DG was being used to charge the battery. Additionally, by comparing the graph of the PSO and the FLC, it can be seen that there is a faster response during the energy transition in the case of the FLC than in the case of the PSO. This faster transition offers stability and prevents disruptions during HRES operations. Therefore, FLC-EMS offers stability and the optimal utilization of the energy resources during HRES operation; it offers reliable energy irrespective of the weather conditions and load fluctuations. The EMS was able to provide energy to the load both in the dry season and in the rainy season. Figure 28a,b show that the FLC-EMS could keep the battery SOC within the desired range of 55% to 80%.

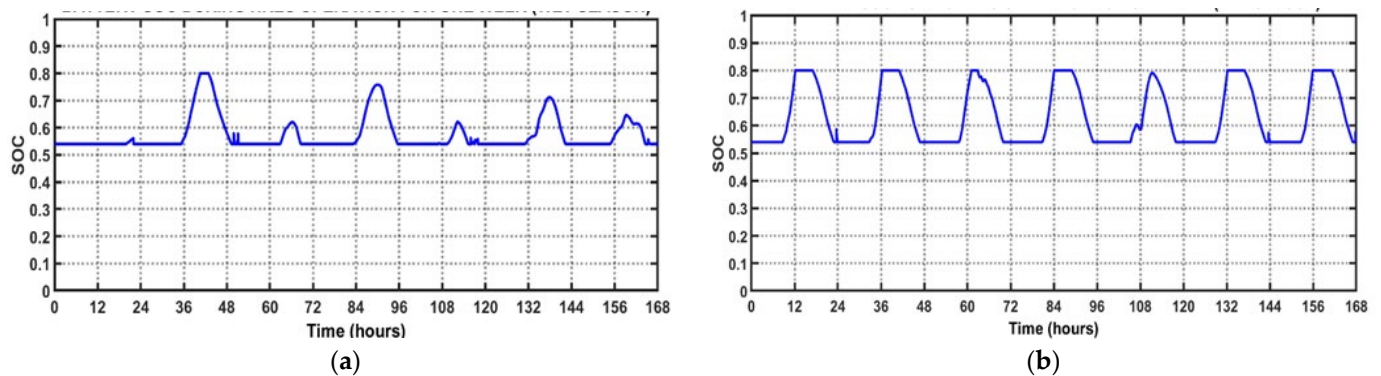


**Figure 28.** State of charge (SOC) for 1 week: (a) January and (b) August.

## 6. Conclusions

This research studied the technoeconomic analysis of providing a hybrid renewable energy system to an off-grid rural community in Nigeria. The investigated HRES includes the PV, wind turbine, battery, and diesel generator, which are used to meet the load demand of an off-grid rural community. The optimal sizing of the HRES equipment was found by using a least-cost perspective approach, which is necessary to ensure the minimum cost of implementation and make the electricity affordable to consumers. This research also developed a fuzzy-logic-controlled energy management system that ensures the optimal operation and reliability of an HRES.

Two scenarios were considered for optimal sizing while using the proposed HRES. In the first scenario, the LCOE for electrifying the off-grid rural community was found to be 0.48 USD/kWh, with the HRES components estimated as 130 kW for PV, 0 kW for wind turbine, 1370 kWh for battery, and 0 kW for DG. However, because of the high capital associated with using the maximum battery capacity, a second scenario, where half of the maximum capacity would be used, was considered. In this latter scenario, the LCOE for electrifying the off-grid rural community by using a hybrid renewable energy system was found to be 1.17 USD/kWh, with the HRES components estimated as 100 kW for PV, 0 kW for wind turbine, 700 kWh for battery, and 25 kW for DG. The results revealed that wind energy could not be considered as an energy source in the two scenarios, because of the low wind speed in the region. Furthermore, the effect of the different seasons was observed on the PV power output. More PV power can be generated in the dry season compared to the wet season. Consequently, more renewable energy was used to meet the demand in the dry season, and more DG power was used to meet the load demand in the wet season.

The FLC-EMS comprised two FLCs, denoted as FLC1 and FLC2. FLC1 manages the battery charging and discharging, while FLC2 manages the DG operation. The FLC-EMS rules were designed on the basis of expert knowledge and were used to schedule the energy sources in order to meet the load demand while prioritizing renewable energy. The controller could switch at any time of operation, as required, to ensure an energy balance between the energy supply sources and the energy demand of the community. For this study, the membership functions of the variables and the FLC rules were constructed on the basis of the operators' knowledge; however, in future work, the parameters of the membership functions can be tuned using PSO or any other optimization algorithm, and the fuzzy rules can be chosen on the basis of the optimization algorithm.

The results from this study can be used as a general overview and a quick feasibility study to determine the technical and economic implications of implementing and operating an HRES in an off-grid rural community in Nigeria.

**Author Contributions:** Conceptualization and methodology, T.A. and H.F.; investigation and data curation, T.A.; writing—original draft preparation, T.A.; writing—review, editing, and supervision H.F. All authors have read and agreed to the published version of the manuscript.

**Funding:** This research received no external funding.

**Institutional Review Board Statement:** Not applicable.

**Informed Consent Statement:** Not applicable.

**Data Availability Statement:** Not applicable.

**Acknowledgments:** The authors would like to thank the Japan Africa Dream Scholarship (JADS) Program, for providing financial support for this research. The authors appreciate ACOB Lighting Technology Limited for acquiring the case-study data.

**Conflicts of Interest:** The authors declare no conflict of interest.

## References

1. Stears Data and Sterling. *Nigeria's State of Power 'Electrifying the Nation's Economy'*; Stears Data and Sterling: Lagos, Nigeria, 2022.
2. Nigeria to Improve Electricity Access and Services to Citizens. Available online: <https://www.worldbank.org/en/news/press-release/2021/02/05/nigeria-to-improve-electricity-access-and-services-to-citizens> (accessed on 28 June 2022).
3. Nigeria—Living Standards Survey 2018–2019. Available online: <https://microdata.worldbank.org/index.php/catalog/3827> (accessed on 28 January 2023).
4. Electric Power Sector Reform Act. The Federal Government Press: Lagos, Nigeria, 2005. Available online: <https://rea.gov.ng/wp-content/uploads/2017/09/Electric-Power-Sector-Reform-Act-2005.pdf> (accessed on 29 January 2023).
5. Owebor, K.; Diemuodeke, E.O.; Briggs, T.A.; Imran, M. Power Situation and renewable energy potentials in Nigeria—A case for integrated multi-generation technology. *Renew. Energy* **2021**, *177*, 773–796. [[CrossRef](#)]
6. Advisory PowerTeam, Office of the Vice President. Federal Government of Nigeria in Conjunction with the Power Africa “Nigeria Power Baseline Report, 2015”. Available online: <https://www.yumpu.com/en/document/view/55374330/nigeria-power-baseline-report> (accessed on 18 January 2023).
7. The Challenges with Transforming the Nigerian Power Landscape. Available online: <https://www.pwc.com/ng/en/assets/pdf/power-roundtable-2016.pdf> (accessed on 28 January 2023).
8. Data Catalog. Population Estimates and Projections. Nigeria Population 2021. Available online: <https://datacatalog.worldbank.org/search/dataset/0037655/Population-Estimates-and-Projections> (accessed on 29 January 2023).
9. N. Enterprise Agency. *Solar Report Nigeria Commissioned by The Netherlands Enterprise Agency, 2021*; Netherlands Enterprise Agency: Hague, The Netherlands, 2021.
10. Akhator, P.E.; Obanor, A.I.; Sadjere, E.G. Electricity situation and potential development in Nigeria using off-grid green energy solutions. *J. Appl. Sci. Environ. Manag.* **2019**, *23*, 527. [[CrossRef](#)]
11. *ESMAP Global Photovoltaic Power Potential by Country*; World Bank: Washington, DC, USA, 2020.
12. Ikeagwuani, I.; Bamisile, O.; Abbasoglu, S.; Julius, A. Performance Comparison of PV and Wind Farm in Four Different Regions of Nigeria. In Proceedings of the 1st Asup Unwana National Conference, Unwana, Nigeria, August 2016.
13. Shaaban, M.; Petinrin, J.O. Renewable energy potentials in Nigeria: Meeting rural energy needs. *Renew. Sustain. Energy Rev.* **2014**, *29*, 72–84. [[CrossRef](#)]
14. Relations, E.-I. Renewable Energy: Global Challenges. Available online: <https://www.e-ir.info/2016/05/27/renewable-energy-global-challenges/> (accessed on 18 January 2023).

15. Farzaneh, H. Design of a Hybrid Renewable Energy System Based on Supercritical Water Gasification of Biomass for Off-Grid Power Supply in Fukushima. *Energies* **2019**, *12*, 2708. [CrossRef]
16. Shaqour, A.; Farzaneh, H.; Yoshida, Y.; Hinokuma, T. Power control and simulation of a building integrated stand-alone hybrid PV-wind-battery system in Kasuga City, Japan. *Energy Rep.* **2020**, *6*, 1528–1544. [CrossRef]
17. Liu, Z.; Li, H.; Liu, K.; Yu, H.; Cheng, K. Design of high-performance water-in-glass evacuated tube solar water heaters by a high-throughput screening based on machine learning: A combined modeling and experimental study. *Sol. Energy* **2017**, *142*, 61–67. [CrossRef]
18. Farzaneh, H. Energy Systems Modeling. In *Energy Systems Modeling*; Springer: Singapore, 2019. [CrossRef]
19. Pelland, S.; Turcotte, D.; Colgate, G.; Swingler, A. Nemiah valley photovoltaic-diesel mini-grid: System performance and fuel saving based on one year of monitored data. *IEEE Trans. Sustain. Energy* **2012**, *3*, 167–175. [CrossRef]
20. Yin, C.; Wu, H.; Locment, F.; Sechilariu, M. Energy management of DC microgrid based on photovoltaic combined with diesel generator and supercapacitor. *Energy Convers. Manag.* **2017**, *132*, 14–27. [CrossRef]
21. Xu, L.; Wang, Z.; Liu, Y.; Xing, L. Energy allocation strategy based on fuzzy control considering optimal decision boundaries of standalone hybrid energy systems. *J. Clean. Prod.* **2021**, *279*, 123810. [CrossRef]
22. Lian, J.; Zhang, Y.; Ma, C.; Yang, Y.; Chaima, E. A review on recent sizing methodologies of hybrid renewable energy systems. *Energy Convers. Manag.* **2019**, *199*, 112027. [CrossRef]
23. Anoune, K.; Bouya, M.; Astito, A.; Abdellah, A. Ben Sizing methods and optimization techniques for PV-wind based hybrid renewable energy system: A review. *Renew. Sustain. Energy Rev.* **2018**, *93*, 652–673. [CrossRef]
24. Liu, Z.; Chen, Y.; Zhuo, R.; Jia, H. Energy storage capacity optimization for autonomy microgrid considering CHP and EV scheduling. *Appl. Energy* **2018**, *210*, 1113–1125. [CrossRef]
25. Amer, M.; Namaane, A.; M'Sirdi, N.K. Optimization of hybrid renewable energy systems (HRES) using PSO for cost reduction. *Energy Procedia* **2013**, *42*, 318–327. [CrossRef]
26. Yoshida, Y.; Farzaneh, H. Optimal design of a stand-alone residential hybrid microgrid system for enhancing renewable energy deployment in Japan. *Energies* **2020**, *13*, 1737. [CrossRef]
27. Mohammed, O.H.; Amirat, Y.; Benbouzid, M. Particle Swarm Optimization Of a Hybrid Wind/Tidal/PV/Battery Energy System. Application To a Remote Area In Bretagne, France. *Energy Procedia* **2019**, *162*, 87–96. [CrossRef]
28. Takatsu, N.; Farzaneh, H. Techno-economic analysis of a novel hydrogen-based hybrid renewable energy system for both grid-tied and off-grid power supply in Japan: The case of Fukushima prefecture. *Appl. Sci.* **2020**, *10*, 4061. [CrossRef]
29. Yuan, Y.; Zhang, T.; Shen, B.; Yan, X.; Long, T. A fuzzy logic energy management strategy for a photovoltaic/diesel/battery hybrid ship based on experimental database. *Energies* **2018**, *11*, 2211. [CrossRef]
30. Althubaiti, M.; Bernard, M.; Musilek, P. Fuzzy logic controller for hybrid renewable energy system with multiple types of storage. In Proceedings of the 2017 IEEE 30th Canadian Conference on Electrical and Computer Engineering, Windsor, ON, Canada, 30 April–3 May 2017. [CrossRef]
31. Chaurey, A.; Kandpal, T.C. A techno-economic comparison of rural electrification based on solar home systems and PV microgrids. *Energy Policy* **2010**, *38*, 3118–3129. [CrossRef]
32. Lumpur, K. Techno Economic Analysis Of Stand-Alone Hybrid Renewable Energy System Hanieh Borhanazad Research Project. Master's Thesis, Faculty of Engineering, University of Malaya, Kuala Lumpur, Malaysia, 2013.
33. Hinokuma, T.; Farzaneh, H.; Shaqour, A. Techno-economic analysis of a fuzzy logic control based hybrid renewable energy system to power a university campus in Japan. *Energies* **2021**, *14*, 1960. [CrossRef]
34. Berrazouane, S.; Mohammedi, K. Parameter optimization via cuckoo optimization algorithm of fuzzy controller for energy management of a hybrid power system. *Energy Convers. Manag.* **2014**, *78*, 652–660. [CrossRef]
35. Goudarzi, A.; Li, Y.; Xiang, J. Efficient energy management of renewable resources in microgrids. In *Renewable Energy Microgeneration Systems; Customer-Led Energy Transition to Make a Sustainable World*; Academic Press: London, UK, 2021; pp. 285–321. [CrossRef]
36. Mohamed, M.A.; Eltamaly, A.M.; Alolah, A.I. Sizing and techno-economic analysis of stand-alone hybrid photovoltaic/wind/diesel/battery power generation systems. *J. Renew. Sustain. Energy* **2015**, *7*, 063128. [CrossRef]
37. Kennedy, J.; Eberhart, R. Particle Swarm Optimization. In Proceedings of the ICNN'95—International Conference on Neural Networks, Perth, WA, Australia, 27 November 1995; Available online: [https://www.cs.tufts.edu/comp/150GA/homeworks/hw3/\\_reading6%201995%20particle%20swarming.pdf](https://www.cs.tufts.edu/comp/150GA/homeworks/hw3/_reading6%201995%20particle%20swarming.pdf) (accessed on 28 June 2022).
38. Moghaddam, A.A.; Seifi, A.; Niknam, T.; Alizadeh Pahlavani, M.R. Multi-objective operation management of a renewable MG (micro-grid) with back-up micro-turbine/fuel cell/battery hybrid power source. *Energy* **2011**, *36*, 6490–6507. [CrossRef]
39. Kashefi Kaviani, A.; Riahy, G.H.; Kouhsari, S.M. Optimal design of a reliable hydrogen-based stand-alone wind/PV generating system, considering component outages. *Renew. Energy* **2009**, *34*, 2380–2390. [CrossRef]
40. Johnston, R. Fuzzy logic control. *Microelectron. J.* **1995**, *26*, 481–495. [CrossRef]
41. Goguen, J.A.; Zadeh, L.A. Fuzzy sets. *Inf. Control.* **1965**, *8*, 338–353. [CrossRef]
42. Bai, Y.; Wang, D. Fundamentals of fuzzy logic control—Fuzzy sets, fuzzy rules and defuzzifications. In *Advances in Industrial Control*; Springer: London, UK, 2006; pp. 17–36. [CrossRef]
43. POWER. Data Access Viewer. Available online: <https://power.larc.nasa.gov/data-access-viewer/> (accessed on 18 January 2023).

44. Sun. Power VR L Valve Regulated Lead-Acid Batteries for Cyclic Applications. Available online: <https://www.hoppecke.com> (accessed on 18 January 2023).
45. Amutha, W.M.; Rajini, V. Cost benefit and technical analysis of rural electrification alternatives in southern India using HOMER. *Renew. Sustain. Energy Rev.* **2016**, *62*, 236–246. [[CrossRef](#)]
46. Hiendro, A.; Kurnianto, R.; Rajagukguk, M.; Simanjuntak, Y.M.; Junaidi. Techno-economic analysis of photovoltaic/wind hybrid system for onshore/remote area in Indonesia. *Energy* **2013**, *59*, 652–657. [[CrossRef](#)]
47. Azimoh, C.L.; Klintenberg, P.; Wallin, F.; Karlsson, B.; Mbohwa, C. Electricity for development: Mini-grid solution for rural electrification in South Africa. *Energy Convers. Manag.* **2016**, *110*, 268–277. [[CrossRef](#)]
48. Come Zebra, E.I.; van der Windt, H.J.; Nhumaio, G.; Faaij, A.P.C. A review of hybrid renewable energy systems in mini-grids for off-grid electrification in developing countries. *Renew. Sustain. Energy Rev.* **2021**, *144*, 111036. [[CrossRef](#)]

**Disclaimer/Publisher’s Note:** The statements, opinions and data contained in all publications are solely those of the individual author(s) and contributor(s) and not of MDPI and/or the editor(s). MDPI and/or the editor(s) disclaim responsibility for any injury to people or property resulting from any ideas, methods, instructions or products referred to in the content.